Tectonophysics xxx (2012) xxx–xxx

Contents lists available at SciVerse ScienceDirect

Tectonophysics

journal homepage: www.elsevier.com/locate/tecto

Locating and quantifying geological uncertainty in three-dimensional models: Analysis of the Gippsland Basin, southeastern Australia

Mark D. Lindsay [a,b,*], Laurent Aillères [a], Mark W. Jessell [b,c], Eric A. de Kemp [d], Peter G. Betts [a]

[a] School of Geosciences, Monash University, PO Box 28E, Victoria, 3800, Australia
[b] Université de Toulouse, UPS, (OMP), GET, 14 Av. Edouard Belin, F-31400, Toulouse, France
[c] IRD, GET, F-31400, Toulouse, France
[d] Geological Survey of Canada, 236-315 Booth St. Ottawa, Ontario, Canada K1A 0E9

ARTICLE INFO

Article history:
Received 4 June 2011
Received in revised form 30 March 2012
Accepted 6 April 2012
Available online xxxx

Keywords:
Stratigraphic variability
Gippsland Basin
Implicit 3D modelling
Uncertainty grids
Model suite exploration
Structural geology

ABSTRACT

Geological three-dimensional (3D) models are constructed to reliably represent a given geological target. The reliability of a model is heavily dependent on the input data and is sensitive to uncertainty. This study examines the uncertainty introduced by geological orientation data by producing a suite of implicit 3d models generated from orientation measurements subjected to uncertainty simulations. The resulting uncertainty associated with different regions of the geological model can be located, quantified and visualised, providing a useful method to assess model reliability. The method is tested on a natural geological setting in the Gippsland Basin, southeastern Australia, where modelled geological surfaces are assessed for uncertainty. The concept of stratigraphic variability is introduced and analysis of the input data is performed using two uncertainty visualisation methods. Uncertainty visualisation through stratigraphic variability is designed to convey the complex concept of 3D model uncertainty to the geoscientist in an effective manner.

Uncertainty analysis determined that additional seismic information provides an effective means of constraining modelled geology and reducing uncertainty in regions proximal to the seismic sections. Improvements to the reliability of high uncertainty regions achieved using information gathered from uncertainty visualisations are quantified in a comparative case study. Uncertainty in specific model locations is identified and attributed to possible disagreements between seismic and isopach data. Further improvements to and additional sources of data for the model are proposed based on this information. Finally, a method of introducing stratigraphic variability values as geological constraints for geophysical inversion is presented.

1. Introduction

The quality of three-dimensional (3D) representations of geology is measured by their ability to reliably reproduce the geometry and distribution of essential elements of a geological target. To do this a reliable 3D model needs to reconcile all available geological and geophysical data from a study area (Guillen et al., 2008; Jessell, 2001). Further it is fundamental that the model is able to simultaneously represent geology at the surface (where structural field observations may be more abundant) and at depth (where observations are inevitably less abundant). The quality of input data used to construct geological models, such as bedding, structural fabric orientations or lithological contact information, is intrinsically linked to the quality of the final product. Uncertainties contained within the input data for 3D model architecture can potentially reproduce unreliable geology. The aim of this is paper is to communicate a new method that assesses, locates and visualises the effects of data uncertainty.

Previous studies into the effects of data uncertainty involve methods that assess variability introduced by human or machine during data collection, processing (including data reduction during project upscaling) and interpretation (Bond et al., 2010; Bowden, 2007; Jones et al., 2004; Thore et al., 2002). The solution is often an attempt to reduce the effects of data uncertainty before its integration into the model. In contrast, the method described here follows recent contributions by Caumon et al. (2007), Jessell et al. (2010), Viard et al. (2010) and Wellmann et al. (2010) that assess the final 3D model for geological uncertainty. It is assumed that the input data contains uncertainty and this method does not attempt the difficult task of removing it prior to input. Instead the method provides an assessment of uncertainty after data input and includes a suite of possible 3D models that can be evaluated simultaneously.

The difference between a single realisation, or 'best' model approach and multiple realisations from input data is highlighted by Bond et al. (2010) as the difference between inexperienced and experienced geoscientists. A group of geoscientists of varying experience was asked to interpret a synthetic seismic section. The results of their efforts were assessed, including success in picking seismic horizons correctly, the content and quantity of discussion between

* Corresponding author at: School of Geosciences, Monash University, PO Box 28E, Victoria, 3800, Australia. Tel.: +61 3 9905 4879; fax: +61 3 9905 4903.
E-mail address: mark.lindsay@monash.edu (M.D. Lindsay).

0040-1951/$ – see front matter © 2012 Elsevier B.V. All rights reserved.
doi:10.1016/j.tecto.2012.04.007

candidates and the type and quality of annotations added to interpretations. While better results from the more 'successful' candidates could be attributed to their experience in the geoscience field, it was also their experience that led them to acknowledge that finding the 'right answer' with the available information was unlikely. In fact, the assumption amongst the more successful subjects was the interpretation was likely to be incorrect, but with the available data it was the best that could be obtained. The low likelihood of finding the correct answer, or model, from sparse datasets is therefore not a revolutionary concept, rather is it a common assumption within the geosciences. Interestingly, and contrary to this understanding, input data is commonly used to create one optimised or 'best' model by modellers. This study argues that no 'best' model exists and that all members of the model suite are geologically possible. The key is to find the regions of difference between the models.

An interesting direction for this research is to measure data density effects on the model quality (e.g. Putz et al., 2006). Determining which data points assist or retard the calculation of reliable model structures can streamline data input. Further, this type of information can identify which points provide useful geometrical or geological constraints and can help delineate essential data input on this basis. While these effects could be studied using the technique present in this paper, downsampling data points would introduce additional experimental effects that are difficult to characterise within the scope of this introductory study. This research direction is a deserving subject for a separate paper, and is therefore not presented here.

The first section of this paper examines particular aspects of input data sensitivity, identified by Jessell et al. (2010), and uses techniques described in their contribution. It also examines the nature of geological input data and how it is used in 3D modelling applications by describing a method that visualises the location and magnitude of geological uncertainty through a 'geological perturbation' technique. Examples of this technique are provided with both simple and complex geological settings. Simple, synthetic models provide clear examples of how this technique can visualise geological uncertainty in 3D.

The second part of this paper examines a case study from the Gippsland Basin, southeastern Australia to display how this technique can be applied to a natural geological setting. The Gippsland Basin is an offshore geological environment displaying relatively complex geological fold and fault relationships within a mature oil and gas field environment. An assessment of uncertainty is conducted on the Gippsland Basin model, and suggestions are made and carried out to improve model reliability. Analysis into the effects of additional input data is provided, as well as an explanation of how the technique can provide important information to guide field studies and aid the discovery of key localities. Lastly, a use for the data generated by the technique in geophysical inversion is proposed.

2. Geological uncertainty

The process of creating a 3D model begins with the collection of relevant data that will support the creation of a digital representation of geology. The types of data required are varied and the relative importance of each depends on scale (from mine scales to crustal scales), application and target. In practice, however, 3D model construction often suffers from a lack of geological information, independent of scale, due to sparse outcrop limiting field observations and inadequate borehole or geophysical data. This often means that all available data is utilised, regardless of original purpose, application or collection scale (Kaufmann and Martin, 2008; Royse, 2010). Interpretation of geology from geophysics may need to be performed prior to input into a 3D modelling package to better understand regions lacking geological observations, (e.g. Aitken and Betts, 2009). Determining whether the same lithological contact is continuous under cover or determining the morphology of a structure (Fig. 1a) is a

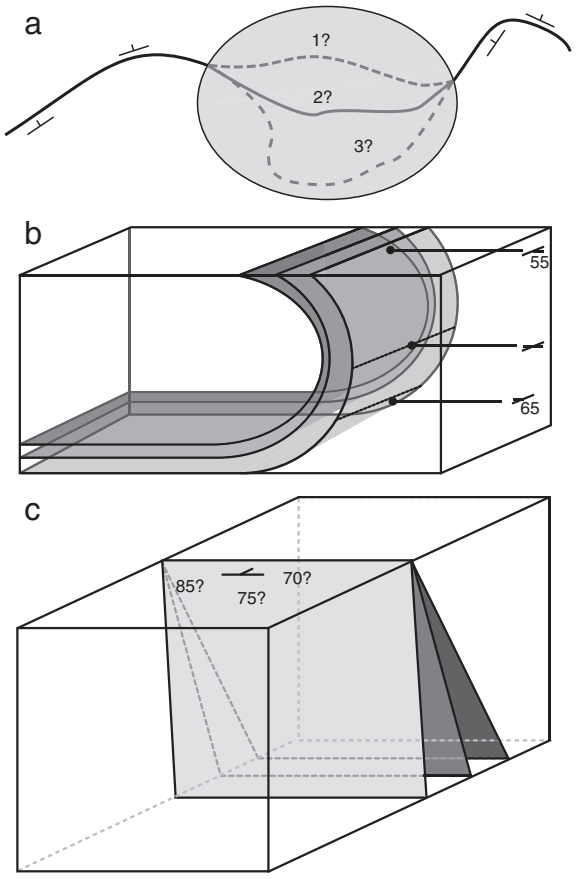

Fig. 1. (a) Most geological mapping requires a degree of interpolation. In this example three possible options (though many more exist) are presented to the geologist, but only one will be recorded. This decision is made by the geologist, often with the benefit of prior knowledge and experience of the terrane. Unfortunately, the other possibilities are lost to others viewing the map, which may more accurately resemble the true geology.(b) Some geological measurements do not completely represent the observed surface. In this example of a recumbent fold limb, a dip measurement of 55° at the surface is reasonable, but fails to convey that the bedding dip angle changes to sub-vertical if taken at the first dashed line(fold axis) and eventually reverses with depth (second dashed line). This situation is also prevalent in poly-deformed terranes.(c) Weathered terranes often require an estimated measurement of a geological surface. When an estimated measurement is entered into a 3D model the resulting geometry can have compounding effects on the model, especially at depth. The location of a geological surface can vary considerably at depth even with a small measurement error at the surface.

decision made using geological expertise and is often aided with the use of geophysical interpretation (Betts et al., 2003; Gunn et al., 1997; Joly et al., 2007).

Forward modelling of geophysical data is often part of 3D model construction workflows, aiding the constraint of geological surfaces in cross-section (Jessell, 2001). The price of using geophysical data to aid geological interpretation in the process of creating a 3D model is the introduction of a possible additional source of uncertainty. Geophysical data ambiguity is not a new issue and has been well covered since Nettleton (1942) began critically assessing the interpretations of his contemporaries. It was recognised in his and further studies that a number of possible outcomes could fit a particular geophysical data set and render any interpretation meaningless without the proper geological controls (Clark, 1983, 1997; Gunn, 1997). Endeavours to remove geophysical ambiguity from geophysical interpretation is a critical component of any related study and is usually performed, often with much effort, by collecting petrophysical data appropriate to the geophysical potential field being utilised (e.g. Joly et al., 2008; Nabighian et al., 2005; Williams et al., 2009).

Inherent uncertainty is not only confined to geophysical data. Uncertainty also needs to be considered when using geological data.

Please cite this article as: Lindsay, M.D., et al., Locating and quantifying geological uncertainty in three-dimensional models: Analysis of the Gippsland Basin, southeastern Austral..., Tectonophysics (2012), doi:10.1016/j.tecto.2012.04.007

Measurements taken when field mapping and drill-core logging are typically 3D observations recorded in a 2D (bedding contacts, fault plane, fold hinge or foliations) or 1D context (lineation or fold plunge). The uncertainty of these measurements and their interpretation can generally be associated with any of the following considerations (Jessell et al., 2010; Jones et al., 2004; Thore et al., 2002; Torvela and Bond, 2010; Wellmann et al., 2010):

- Does the observation represent the geological surface or vector at depth? It is possible that the angle or strike/plunge of a structure varies from the surface measurement to that at depth (Fig. 1b). Additionally, 3D models are often constructed at the regional scale using data collected in detailed field mapping. This requires the downsampling of data to a few 'representative' points that may fail to adequately represent the geological element.
- What impact does scale have on the modelled structures? Downsampling of data also has implications related to model scale. Orientation measurements used in the calculation of the implicit potential field and subsequent modelled geology may have been obtained from local geological structures, such as parasitic folds or fault splays. Uncertainty can be introduced if the local structure cannot be adequately resolved in detail when the model is calculated with regional scale parameters. The inverse is also true, where regional scale data (such as seismic or gravity) is used to generate small-scale structures.
- Are bedding contacts easily discernible? Determining the orientation of bedding planes requires a degree of estimation for both strike and dip if bedding contacts are not clear. For example some geological terranes are weathered to such a degree that confidence in the measurement is low. Any error in estimating the dip of these contacts can have problematic effects, as different orientations have increasing ranges of geometrical possibilities with increasing depth (Fig. 1c).
- Do existing theoretical models affect input data? Current understanding and hypotheses concerning a particular geological terrane can oversimplify geological reality. Interpretations may underestimate the complexity of the geology. The resulting model may misrepresent the geology, resulting in an unreliable product. Again, the inverse is also true, where over-interpretation may result in a model that is too complex.

Field data may also be vulnerable to error if the modelling is not being performed by the field geologist. Critical knowledge of the terrane and knowledge of the reliability of measurements may be lost. Processes have been developed to reduce this effect by introducing workflows that encourage the field geologist to record levels of confidence in measurements (Jones et al., 2004). Normally, implicit knowledge of the terrane remains difficult to transfer to others as it is tacit knowledge (Jones et al., 2004; Polanyi, 1962). This includes knowledge of the interpretive and mapping skills of the geologist and a priori information that is taken into the field. Measurements may be taken with a particular preconceived model topology in mind resulting in biased observations being recorded.

3. Implicit 3D geological modelling

A requirement of the technique described here is to use an implicit 3D modelling application. The advantage of implicit modelling over other techniques (such as explicit techniques) is the speed at which models can be re-calculated with additional data to produce repeatable and objective results. Explicit modelling techniques require the operator to manually add vertices to construct geological structures. Some automated processes, such as Discrete Smooth Interpolation (DSI) (Mallet, 1992), are available to assist in creating geologically reasonable structures, but essentially the explicit methods require significant operator input to produce a feasible model. Consequently, a significant amount of time is required to produce each model and the results are not repeatable. Explicit techniques are not appropriate in terms of time and repeatability as many models are being produced from a single data set in this study. In contrast, implicit modelling features are beneficial to the method, allowing automated model calculation, rapid model realisation and repeatable results. An implicit geological modelling application, 3D Geomodeller (www.geomodeller.com), was chosen as the modelling and simulation platform for this study.

3D Geomodeller utilises the 'implicit potential field' method to construct geological interfaces as implicit surfaces (Lajaunie et al., 1997). In this context, 'potential field' describes a scalar function from which geology is generated. The objective is to model geological interfaces based on three principles: (i) geological interfaces define the contact between geological formations; (ii) structural field data orientations (i.e. strike and dip) sampled within geological formations are used to model the interfaces separating formations and (iii) all modelled interfaces are part of an infinite set of surfaces that are aligned with the orientation of the implicit potential field (Calcagno et al., 2008) (Fig. 2a–c).

Certain requirements are needed for this form of modelling to take place. A stratigraphic column must be specified and formations within the column must have at least one location data point and one orientation data point before they can be calculated. Geology is calculated from the implicit potential field that is a scalar function $T(p)$ of any point $p=(x, y, z)$ within 3D space where T can represent a relevant geological process that can be assigned a numerical value (i.e. time of deposition or geological age). The implicit potential field is an isosurface of the scalar field, and a geological contact can be considered to be where reference isovalues change from one lithology to another. The implicit potential field is interpolated from cokriging of the geological contact (contact location) and orientation (contact geometry) data and allows the

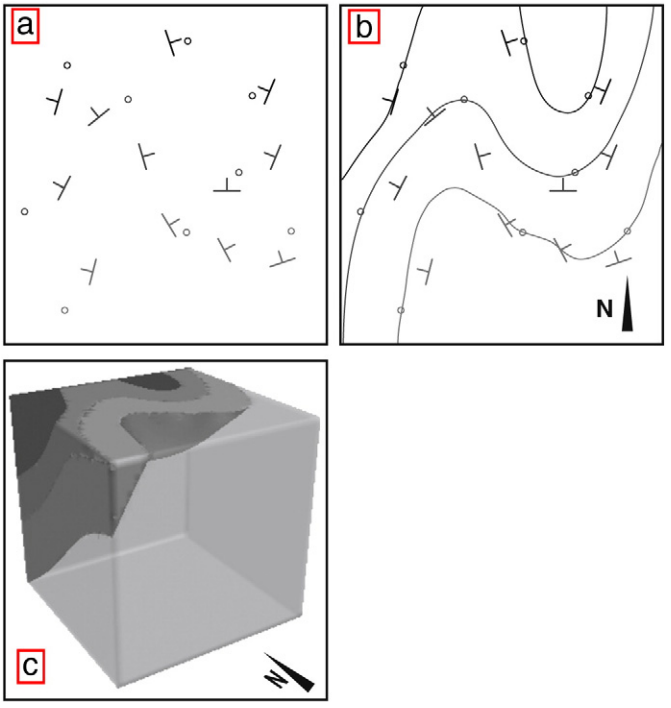

Fig. 2. Example of creating a geological surface in an implicit modelling environment. 3D Geomodeller is used in this example. (a) Digitised geological map of three formations in black, dark grey and light grey. Outcrop points are depicted as circles, dip and strike are depicted with the standard convention. (b) Interpolated geological map determined by the potential field method. The solid lines represent contacts between the three formations. Note how both contact and orientation (strike and dip) points are honoured to produce an antiform–synform pair. (c) 3D representation of the input data.

Please cite this article as: Lindsay, M.D., et al., Locating and quantifying geological uncertainty in three-dimensional models: Analysis of the Gippsland Basin, southeastern Austral..., Tectonophysics (2012), doi:10.1016/j.tecto.2012.04.007

determination of geological interfaces that honour the input data (Lajaunie et al., 1997).

The stratigraphic column defines the geological units being modelled, which can then be sorted into geological 'series' to represent a group of geological formations (Fig. 3a). Each series has an implicit potential field calculated separately to the others. The interaction each series and implicit potential field has with other series and implicit potential fields is defined by its chronological position and behaviour exhibited with respect to older formations. Behaviour is set as either an 'erode' relationship, where older units are cross-cut or truncated, or 'onlap' where a series is allowed to be present if space permits without modification of the underlying older series (Calcagno et al., 2008). Each geological unit has a numerical attribute, that allows identification of the stratigraphic unit (Fig. 3a) at a given *X*, *Y*, *Z* co-ordinate. Faults are interpolated in a similar manner to lithologies. Fault-specific orientation data defines the fault dip and fault trace data points define fault location. The age of a fault is defined in two ways: (i) by interactions between faults and geological units (Fig. 3b) and (ii) faults and other faults (Fig. 3c). A fault may only affect some units in the stratigraphic column and can also terminate on another fault.

Model topology is defined by assigning both chronological and relationship parameters between geological units and faults in the model. The chosen topology is probably only one of multiple possible versions that exist for the terrane under study, so the choice of relationships becomes a subjective decision made by the geologist. Unfortunately, multiple topologies cannot be explored simultaneously at this stage, but by changing these relationships manually and recalculating the model, different topologies can be realised to test various scientific hypotheses for geological feasibility.

4. Method

Rather than attempt to remove uncertainty from the input data, this paper assumes that the input data contains uncertainty and attempts to simulate its effects through 'geological perturbation'. Perturbing a set of structural field measurements allows different model possibilities to be generated and assessed. This 'geological perturbation' method attempts to simulate uncertainty by randomly adjusting observed strike and dip measurements within a range of 10° to produce a suite of 'what-if?' scenarios. This process is analogous to an 'en-masse' field mapping survey by a large number of geologists. The maps produced by the end of the survey all tend to look similar, but differ slightly in various ways due to geological uncertainty. In addition, the geologists may have focussed on some areas more than others or taken measurements from different fabrics at the same outcrop. The benefit is that collectively these maps may produce interpretations that change our geological understanding of the study area.

4.1. Calculating, quantifying and visualising model uncertainty

By adjusting strike and dip values of the input orientation data we can reveal the location and magnitude of uncertainty contained within the model. We define uncertain regions as those where the location, morphology or orientation of geological structures are different between models. Geological structures that can vary include fault surfaces, folds or lithological contacts in terms of their geometry, orientation, scale, shape and position. It is considered that an increase in uncertainty is inversely proportional to the reliability of the model, so it is critical to understand where these regions are. Uncertainty

a

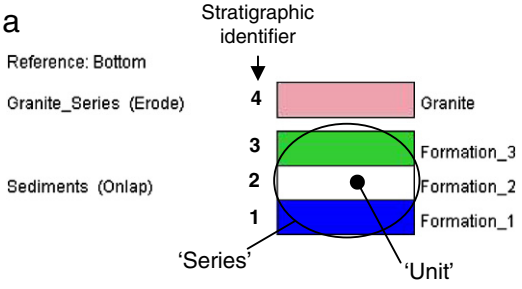

b

	Fault 1	Fault 2	Fault 3
Granite		✓	
Sediments	✓	✓	✓

c

Stops on	Fault 1	Fault 2	Fault 3
Fault 1		✓	
Fault 2			
Fault 3	✓	✓	

Fig. 3. Example of possible relationships between different geological elements. (a) Stratigraphy showing three conformable ('onlap') sedimentary units in one series that are cross-cut ('erode') by a younger granite unit. Note how the numerical attribute is assigned in ascending geochronological order. (b) Fault–stratigraphy relationship matrix defining which series are faulted by which fault. This matrix shows that Fault 2 must be a late fault as it affects all series defined in the pile (and therefore younger the Faults 1 and 3 which only affect the older 'Sediments' series). Faults 1 and 3 must be older than the granite, but younger than the sediments. (c) Fault–fault relationship matrix defining how faults 'stop on' or are cross-cut by other faults. This matrix only describes geometrical relationships between faults and not necessarily their relative ages.

Please cite this article as: Lindsay, M.D., et al., Locating and quantifying geological uncertainty in three-dimensional models: Analysis of the Gippsland Basin, southeastern Austral..., Tectonophysics (2012), doi:10.1016/j.tecto.2012.04.007

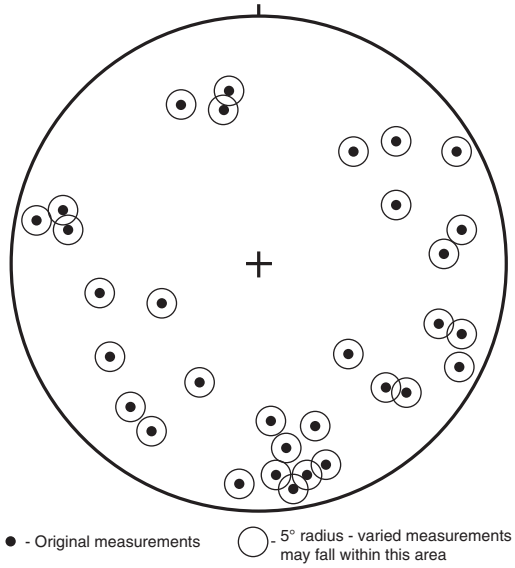

Fig. 4. Stereonet plot comparison of original, or initial, measurements and a five degree zone of possibility circling each original measurement. The zone indicates where varied measurements may be plotted after being subjected to uncertainty simulation.

information can be used to aid subsequent data collection activities to further constrain the model and increase reliability.

The visualisation and processing of uncertainty data is achieved by calculating a 3D uncertainty grid: a record of stratigraphic units found at discrete locations within each model, calculated from perturbed measurements. Locations within each model are described within the grid by an *X*, *Y* and *Z* reference. Once processing has been performed, a function describing stratigraphic variability is used as a proxy for uncertainty during visualisation and is assigned to the appropriate location.

4.2. Procedure

Four steps are required to produce, process and visualise an uncertainty grid.

A. Construction of 3D model
   The process begins with the construction of a reference model, normally the final product in most workflows. All available and relevant data should be used to produce this model. Critical to this technique is that strike and dip orientation data is used as: (i) they are required by the implicit potential field technique and (ii) they are the components that are perturbed to allow varied models to be calculated.
B. Variation of geological orientation data
   The model is perturbed by varying the input orientation data strike and dip measurements (related to foliations and faults) by $\pm 5°$ from original reference model measurements. Five degrees was chosen as a reasonable amount of variation that may be observed between measurements taken by different geologists, especially in weathered, covered or highly-deformed terranes where the relationship between larger and smaller scale structures is not clear. A

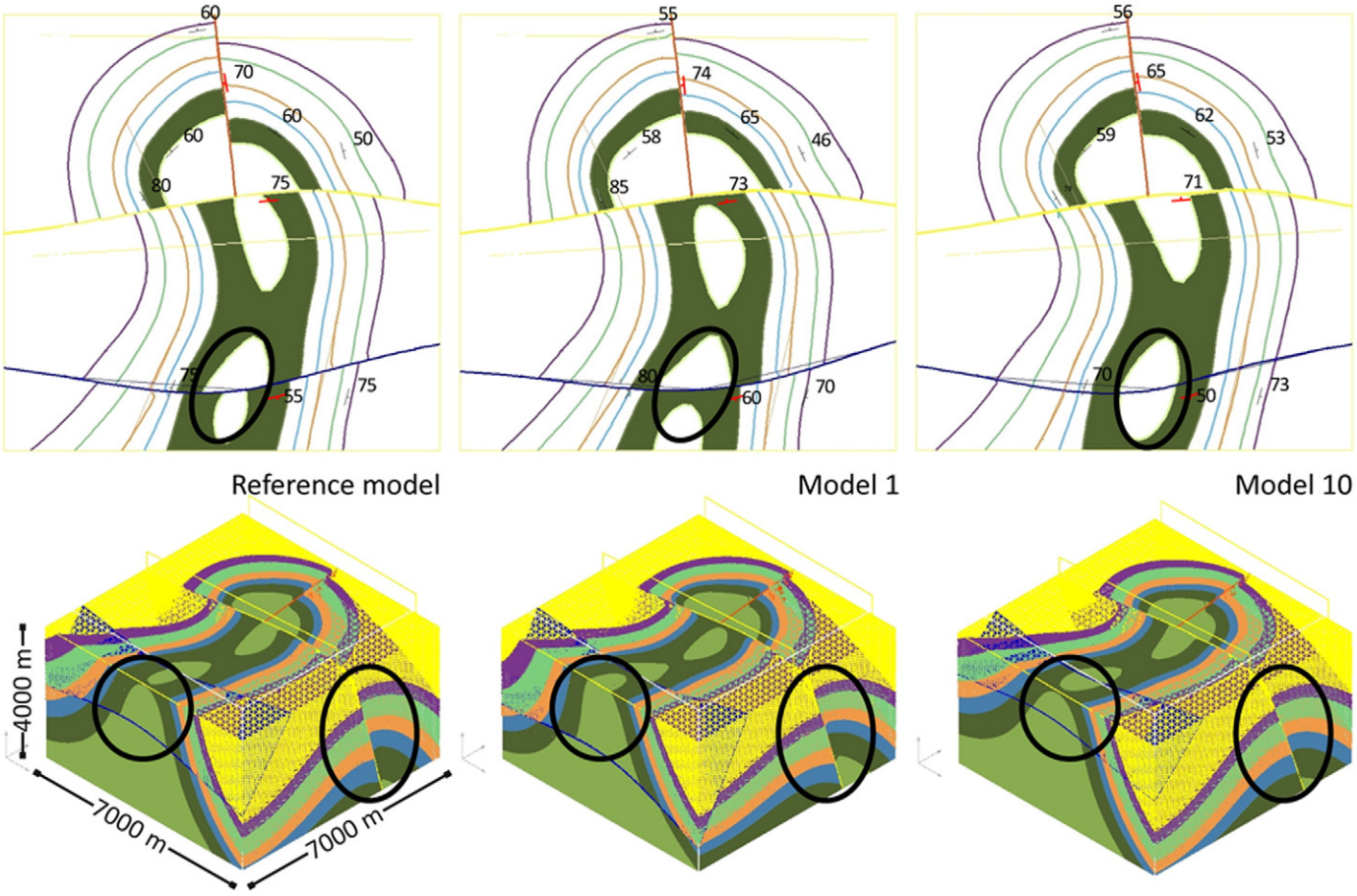

Fig. 5. Three synthetic models constructed from a perturbed data set. The 'Reference model' contains the original strike and dip observations. The top row of images shows a surface map view of the geology interpolated by a potential field method (Section 3 and Fig. 2a–c). The bottom row of images shows an oblique view of the corresponding 3D block models. The black circles show regions of noteworthy difference between each model on both map and block diagram views. The most important differences are associated with faulting structures.

Please cite this article as: Lindsay, M.D., et al., Locating and quantifying geological uncertainty in three-dimensional models: Analysis of the Gippsland Basin, southeastern Austral..., Tectonophysics (2012), doi:10.1016/j.tecto.2012.04.007

stereoplot comparison of synthetic and varied measurements is shown in Fig. 4. Any number of perturbations can be calculated and is restricted only by the power and storage space of the computing platform. In this study, each model suite contains 100 perturbed models and the reference model (101 models in total).

C. Calculation of model suite and model interrogation
Each perturbed model is re-interpolated using the implicit potential field method to accommodate the new, varied orientation input data (Fig. 5). Next, each model is interrogated to collect stratigraphic data at specified X_i Y_i and Z_i. The interrogation process is performed within a given set of parameters along each axis (in UTM projection metre units): an initial co-ordinate (X, Y, Z); a final co-ordinate (X', Y', Z') and a sampling frequency (X_n, Y_n and Z_n). The sample interval along each axis can then be determined and the cell size of the uncertainty cube can be defined (X_s, Y_s, Z_s) (1). If required, volume and area of a particular formation or uncertainty region within the model can be determined, within the constraints of the cell size.

$$[X_s Y_s Z_s] = \frac{\left(\left[X'Y'Z'\right] - [XYZ]\right)}{[X_n Y_n Z_n]} \quad (1)$$

The process is able to determine a stratigraphic unit within the model at each sample location (Fig. 6). The detected stratigraphic unit is returned as a simple integer, the value of which represents its relative location within the stratigraphic column (the 'stratigraphic identifier' or stratigraphic ID — see Fig. 3a). A value of "1" represents the 'basement' or base formation, with values increasing with each successive overlying formation. The next model is interpolated and the interrogation process is repeated using the same sampling parameters with the results concatenated to the uncertainty grid. The process is repeated for the remaining model perturbations. The result is a grid of stratigraphic units describing a sample of each individual model (Table 1).

D. Quantification of uncertainty cube using stratigraphic variability
Visualisation of model uncertainty is now possible by importing the uncertainty grid into a 3D visualisation package. This technique uses gOcad® for this purpose. Locations that show different possible stratigraphic units can be identified by making manual comparisons between each model perturbation, but doing so in this qualitative manner is time-consuming and difficult. A quantitative approach is more time effective, easier and offers more information about the magnitude and variability of uncertainty. The concept of stratigraphic variability has been developed to meet this requirement. Stratigraphic variability is intended to serve a dual purpose by describing model uncertainty spatially and useful for further analysis by providing a value that is statistically valid.

In a simple sedimentary sequence the stratigraphic unit identifiers could be considered ordinal data, with each number representing the relative position of each stratigraphic unit. Ordinal data requires that the number set is ranked, or ordered, so that appropriate statistical treatment can be applied. The presence of igneous units, such as a granitoid, complicates this definition. The depth location of younger granitoids within an older sedimentary sequence can violate the definition of ordinal data where the granitoid cross-cuts or intrudes older units. In other words, the units are not ranked from oldest (basement) to youngest (cover) everywhere in the model if units are intruded or cross-cut by younger granitoids at depth, and therefore can no longer be treated as ordinal data. The number sequence is no longer ordered if based on stratigraphy and the assigned geological evolution of the model. The technique treats the sampled data in this technique as categorical to avoid using inappropriate statistical measures. Each number represents a description of an individual stratigraphic unit, and not a relative position, so categorical values can only be treated in a limited number of ways as compared to continuous or ratio data types (Agresti, 2007; Davis, 2002). Data descriptors such as mean and standard deviation, while yielding results, are meaningless when generated from categorical data and are only useful when indicating relative magnitudes of uncertainty. However, the mode of the generated data does produce values that adequately describe both an optimal model and proportions representing variation.

Stratigraphic variability is composed of two separate values (2). The first represents the number of possible stratigraphic units (L) that exist at a given point. Only the stratigraphic units that exist at that point (i.e. the unique values) are counted. For example, if stratigraphic units '1', '2', '4' and '7' were sampled from a location then L has a value of 4.

$$\begin{aligned} L &= |S| \\ S &= \{I_1, I_2, \ldots I_n\} \end{aligned} \quad (2)$$

where I is a unique number within set S. S is a set of integers representing all possible stratigraphic units, at a given point, within the nth model of the model suite.

The number of stratigraphic possibilities by itself does not completely describe uncertainty data as it does not accommodate the frequency of variation possible at each location. The second

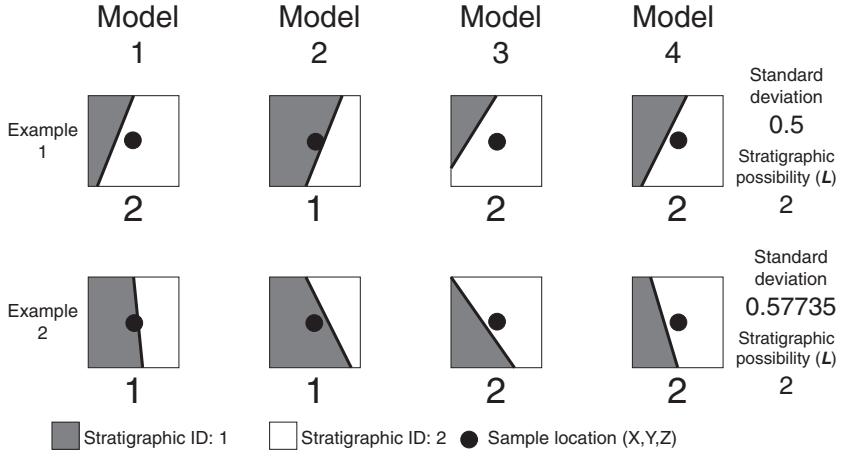

Fig. 6. Example of model uncertainty. Here a standard deviation is used as a relative measure of variability and stratigraphic range (L) refers to number of possible stratigraphic units detected by this technique at this location.

Please cite this article as: Lindsay, M.D., et al., Locating and quantifying geological uncertainty in three-dimensional models: Analysis of the Gippsland Basin, southeastern Austral..., Tectonophysics (2012), doi:10.1016/j.tecto.2012.04.007

Table 1
Sample of the uncertainty grid. Coordinates of the sample location are given on the left-hand side, the results are given on the right-hand side of the table. In the model columns, 'Ref' refers to the reference model and '1, 2, 3, 4…' etc. refer to successive model perturbations.

Coordinates			Model										
X	*Y*	*Z*	Ref	1	2	3	4	5	6	7	8	…	*n*
492,630	5,731,250	−3000	8	8	8	7	8	8	8	8	8	…	8
492,630	5,731,250	−3500	7	7	7	7	7	7	7	7	7	…	7
492,630	5,731,250	−4000	7	7	7	7	7	7	3	7	7	…	7
492,630	5,731,250	−4500	3	3	3	3	3	3	3	3	3	…	3
492,630	5,731,250	−5000	3	3	3	3	3	3	3	3	3	…	3
492,630	5,731,250	−5500	6	3	3	6	3	3	6	3	3	…	3

part of stratigraphic variability determines the degree of frequency, *P*. *P* is calculated by determining the proportion of models that do not equal the mode stratigraphic unit, at a particular location, across the model suite (3).

$$P = \frac{|X \neq Mode(S)|}{|M|} \tag{3}$$

where *X* is a model location with an associated stratigraphic unit and *M* is the model suite. The 'mode stratigraphic unit' is the most common stratigraphic unit across the model suite for a particular *X*, *Y*, *Z*-defined location. For example, if at location *X*: 590,000, *Y*: 610,000 and *Z*: −4500 the distribution of detected stratigraphic units across 100 models was Unit 1: 5, Unit 2: 55, Unit 3: 23 and Unit 4: 17, the stratigraphic mode unit would be 'Unit 2' (55 occurrences). The mode stratigraphic unit is not the stratigraphic unit that is detected from the initial model.

For example, suppose the mode stratigraphic unit for a given location in the model suite is '4'. A *P* value of 0.07 would indicate that 93% of the models in the model suite also exhibit the same stratigraphic unit ('4') and 7% differ from '4' at that location. This method uses a percentage differing from the mode for two reasons: (i) this information describes the frequency of variability between models and (ii) it also provides a value that increases with variability, creating a difference between locations where *L* is equal, but the stratigraphic variability differs. Fig. 7 shows a sample from an uncertainty cube generated from Gippsland Basin data demonstrating why both *L* and *P* values are required. It shows that *L* and *P* values, for a given location, display a loose trend of increasing proportions different to the mode with increasing stratigraphic possibility. There is a degree of variability present, especially for lower magnitudes of stratigraphic possibility. Therefore the property needs to accommodate the amount of lithological variation observed across the model suite for a given location to adequately describe the associated uncertainty. As *L* represents the number of possible stratigraphic units detected at a given location across the model suite, the number of stratigraphic units defined in the stratigraphic pile should also be considered. For example, $L = 4$ indicates relatively less uncertainty in a stratigraphic pile of 20 units than a pile with five units. *L* can be normalised by the total number of stratigraphic units defined in the pile for the purposes of comparing model suites based on different stratigraphic piles. The pre-normalised value is kept intact for this study to retain the explicit description of stratigraphic possibilities.

Uncertainty can be described in better detail if both *L* and *P* values are used. For example, values $L = 3$ and $P = 0.14$ describe a location within the model suite where three different stratigraphic units have been detected and 86% of the models displayed the same stratigraphic unit as model suite mode for that location. These values indicate a moderate level of uncertainty in this location as there are three stratigraphic possibilities, but most of the values represent the mode. In contrast, $L = 6$ and $P = 0.37$ indicate a relatively high level of uncertainty, as there are six possible stratigraphic units and only 63% of models display the model suite mode value for that location. The benefit of using both values allows us to delineate regions with a particular *L* value according to *P*, revealing more detail about the spatial characteristics of model uncertainty. Using *L* and *P* values separately or in combination aids visualisation and model queries. Thresholds can be using either *L* or *P* values assigned to colour maps or used in voxet generation to better describe model uncertainty to the operator.

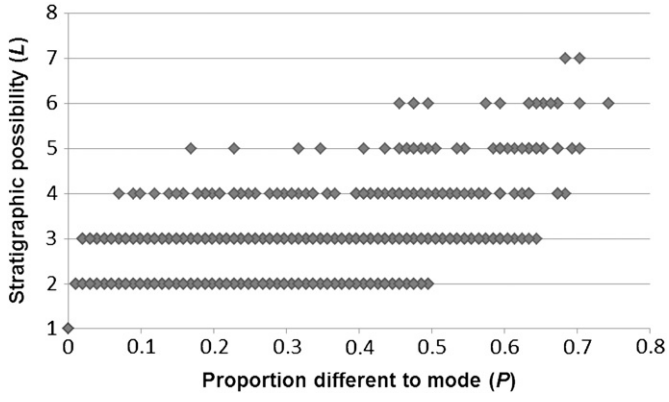

Fig. 7. Plot of *P* versus *L* values, sampled from 15,890 Gippsland Basin data locations. A positive trend is observed, but no correlation ($R^2 = 0.082$). It is clear that both stratigraphic possibility and mode proportion need to be included for the property to be useful as they represent different aspects of uncertainty. For example, an *L* value of '4' yields *P* values between 0.170 and 0.683. Both locations show 4 stratigraphic possibilities and but differ greatly in the amount of variability. Note that the point at (0,1) represents all locations displaying no uncertainty (no difference to the mode and only one stratigraphic possibility).

5. Methods of visualisation

Visualisation of stratigraphic variability as a proxy for uncertainty reveals important aspects of the 3D model and input data. Uncertain regions can be easily located and identification of particular uncertain geological components of the model can be performed. A coincident representation of uncertainty has been chosen, where both modelled geology and associated uncertainty are displayed simultaneously (MacEachren et al., 1998). Different aspects of uncertainty can be revealed using either point data or voxet volumes. Voxets are a set of regularly-spaced voxels (or volume elements) that present data as volumes, rather than as polygons. Wellmann and Regenauer-Lieb (2011) use a similar voxet-based method where information entropy values are assigned to individual voxels. The information entropy property displays the amount of information that is missing from each location, restricting the full prediction of the system.

Magnitude of uncertainty is useful to identify particular uncertain components of the model. In Fig. 8a–c we have assigned a blue-white-green-yellow-red colour map to stratigraphic variability values. Low uncertainty is associated with the blue points and high uncertainty with the red points. The location and magnitude of model uncertainty quickly become evident. Points displaying no uncertainty have been made transparent to aid visualisation. High uncertainty is associated with the fault intersections of the northern east–west thrust fault and the north–south thrust fault. *L* values of five and six have been calculated in this region, particularly at depth. These regions represent the highest geological variability across this model suite. This can be explained by the combined effects of three attributes, fault displacement, fault orientation constraints and bedding orientation

Please cite this article as: Lindsay, M.D., et al., Locating and quantifying geological uncertainty in three-dimensional models: Analysis of the Gippsland Basin, southeastern Austral..., Tectonophysics (2012), doi:10.1016/j.tecto.2012.04.007

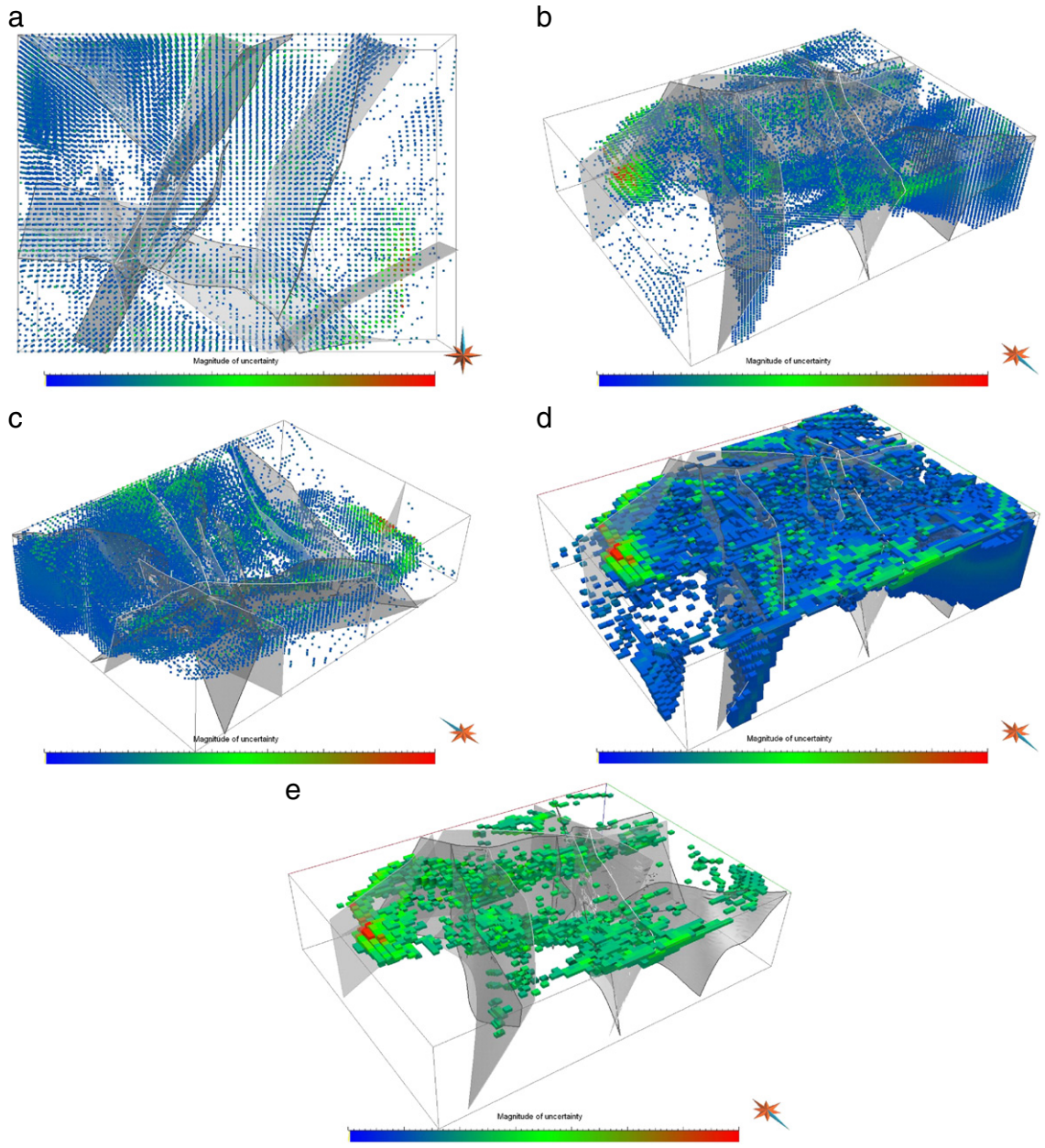

Fig. 8. Comparison of the different visualisation techniques used in the study (VE = ×4) showing the location and magnitude of uncertainty associated with a selection of major faults. Fault borders are shown with alternating border colours to aid differentiating surfaces. Magnitude of uncertainty is displayed using a blue (low values)-green (medium values)-red (high values) colour map. (a) Plan view of model uncertainty (using stratigraphic variability values) using point data. (b) Oblique view of model from above and the northeast using point data. (c) Oblique view of model from above and the southwest using point data. (d) Oblique view of model from above and the northeast using a voxet volume to show stratigraphic variability values, excluding the first 25 percentiles. (e) Oblique view of model from above and the northeast all cells with an L value ≥ 2. (For interpretation of the references to colour in this figure legend, the reader is referred to the web version of this article.)

constraints. Variation in stratigraphic displacement across the fault plane allows more lithological variation as the fault plane orientation changes between models. Each modelled fault is described by one fault orientation measurement. No other measurements assist constraint of the fault surfaces, so when the fault orientation measurements are varied, the fault plane orientation varies freely. Bedding orientation measurements also affect the geometry of bedding surface intersection with the fault surface. Each lithology is defined by limited orientation measurements, therefore a high degree of orientation variation is allowed. The combined effects of sparse data, associated with fault and bedding orientation parameters, have produced a region of high uncertainty.

Uncertainty volumes can be calculated to describe the model, a procedure similar to resource volume calculations (Fig. 8d–e) (see Singer and Menzie, 2010). Volume calculations can help identify areas of high uncertainty similar to the point data technique described above, but are also useful to compare different sets of input data according to uncertainty volume. One application of this technique is to measure how model uncertainty changes with additional orientation measurements.

6. Uncertainty in the Gippsland Basin

The Gippsland Basin in southeastern Australia has been used as a case study to demonstrate the utility of determining, quantifying and assessing 3D model uncertainty. During construction of this model (Fig. 9a–b) it was found that additional information was needed to reduce uncertainty located in certain regions. Two model suites

Please cite this article as: Lindsay, M.D., et al., Locating and quantifying geological uncertainty in three-dimensional models: Analysis of the Gippsland Basin, southeastern Austral..., Tectonophysics (2012), doi:10.1016/j.tecto.2012.04.007

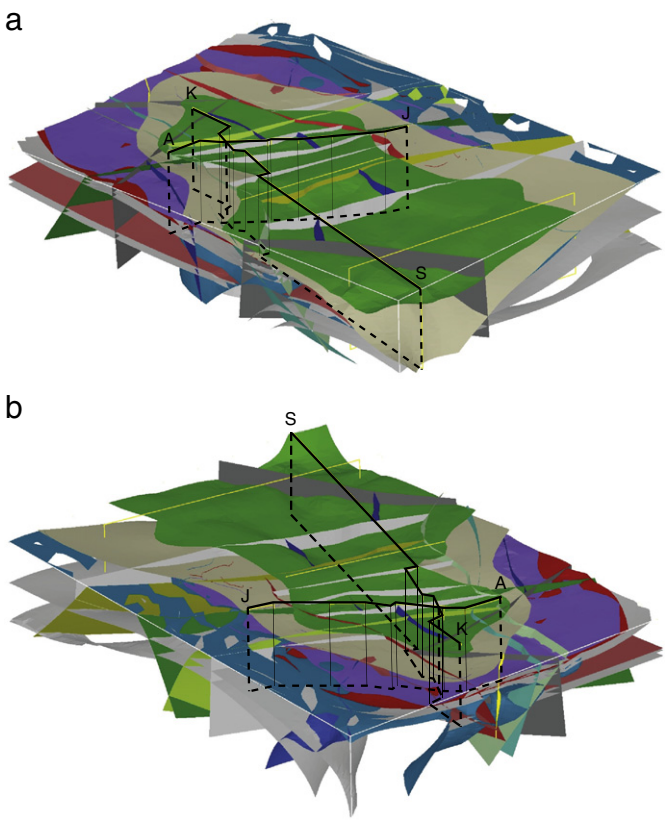

Fig. 9. 3D block diagram of the Gippsland Basin, viewed from the southeast (a) and northwest (b). These images show surfaces rather than volumes so aspects of the model architecture can be more easily viewed. Locations of seismic sections A–J and K–S used in model construction are shown.

are presented, Case Study A and Case Study B. Both model suites were constructed using information provided by Geoscience Victoria (Department of Primary Industries) and Geoscience Australia. Case Study A was constructed using all information and only the interpreted seismic sections K–S taken from the interpretation of Moore and Wong (2002). Case Study B uses the same input data, but includes all available seismic section information from the Moore and Wong (2002) study (seismic sections K–S and A–J). The results show how additional information can reduce uncertainty and serves to improve model reliability.

The models created in the A and B case studies are a simplification of what could be modelled and only major stratigraphic units and faults have been included. We suggest that presenting low fidelity models provides a more effective method in which to display our technique. The geology is therefore described in terms of what has been input into the model, and does not include every possible unit observed in the Gippsland Basin region. The input stratigraphic unit descriptions, relationships and adaption for model input are shown in Fig. 10. The fault networks have been defined according to fault relationships described in the following section.

6.1. Background geology

The Mesozoic to Cenozoic Gippsland Basin is a mature oil and gas field located in southeastern Australia that hosts brown coal deposits and is prospective for CO_2 sequestration (Cook, 2006; Rahmanian et al., 1990). The basin extends from an onshore setting around Western Port Bay offshore into Bass Strait and includes the Melbourne, Bass, Tabberabbera, Kuark and Mallacoota Zones of the Palaeozoic Lachlan Fold Belt (LFB) (Willman et al., 2002). The 80 km by 400 km depocentre trends asymmetrically east–southeast and is underlain by Palaeozoic basement (Moore and Wong, 2002; Rahmanian et al., 1990).

The basement unit for these models is labelled as Ordovician sediments, a collection of various units forming the same basement in the seismic interpretation of Moore and Wong (2002). Overlying the basement unit is the Permian sediments and igneous unit series, a representation of various Permian and Jurassic sedimentary and igneous units (Schmidt and McDougall, 1977).

Sedimentation during the Cretaceous resulted two in distinct units, the volcaniclastic Strzelecki Group, generally regarded as economic basement (Haq et al., 1987), and the lacustrine and marginal-marine quartose-derived Latrobe Group (Moore and Wong, 2002; Veevers, 1986; Veevers et al., 1991). The Latrobe Group is the primary target for oil and gas (Rahmanian et al., 1990) and comprises the Emperor, Golden Beach and Cobia Subgroups (Bernecker and Partridge, 2001; Moore and Wong, 2002). The Emperor Subgroup lacustrine sediment deposition was primarily controlled by early rift-related north–east trending faults over the northern and central parts of the basin (Bernecker et al., 2001; Smith et al., 2000). The western edge of the Cobia Subgroup is considered to be bounded by the Wron Wron Fault System (Moore and Wong, 2002). The Seaspray Group and the Angler Subgroup resulted from further thermal subsidence and marine transgression during the Oligocene (Holdgate et al., 2002; Mitchell et al., 2007). The Angler subgroup forms the base of the Seaspray Group and is characterised by calcareous mudstones and marls (Gallagher et al., 2001).

Moore and Wong (2002) describe the complex fault interactions in the Gippsland Basin as sets of older, straighter basement faults with similar orientations displaced by younger faults with varied orientations. The relationship between basement and younger faults is attributed to a competency contrast between the more rigid basement and softer overlying basin sediments. Two regions of young faults can be observed. The north and west fault sets typically trend northeast–southwest and exhibit steeper dip angles and may have been active as late as the Late Oligocene to Early Miocene. The western faults trend east to west and show possible Quaternary reactivation (Gray and Foster, 1998).

6.2. Input data

The input data used to construct the Gippsland Basin models were taken from the sources listed in Table 2 and shown in Fig. 11. Seismic data was acquired through a combination of Geoscience Australia and company surveys, including those from Esso, Petrofina and Shell. The average internal velocities used to processing the data were: sea water (1480 ms^{-1}); Seaspray Group (2800 ms^{-1}), Latrobe Group (3400 ms^{-1}), Golden Beach/Emperor/Cobia Subgroups (3900 ms^{-1}) and Strzelecki Group (3900 ms^{-1}). A combination of well ties (listed above each well location in Fig. 12) and breaks in seismic property was used to identify seismic reflectors. The seismic interpretations shown in Fig. 12 were digitised from Moore and Wong (2002). Sections A–J were not included in Case Study A, but were included in Case Study B in the attempt to improve model reliability after uncertainty assessment was performed. Geophysical potential field interpretation was performed to identify faults. Both gravity and magnetic data sets were used in combination to identify steep gradients in the geophysical response (Fig. 13). Steep geophysical gradients suggest a rapid change in geophysical character perpendicular to the gradient direction and can infer the presence of a geological interface (Clark, 1997; Grant, 1985). Isopach and bathymetry data was used to create datasets of 3D interface points to aid the interpolation of the top of the Seaspray, Latrobe and Strzelecki groups and the Ordovician sedimentary successions (Fig. 11). Isopach data was supplied by Geoscience Victoria. A large proportion of input geological orientation data was interpreted from both geophysical potential field interpretation and seismic section.

Please cite this article as: Lindsay, M.D., et al., Locating and quantifying geological uncertainty in three-dimensional models: Analysis of the Gippsland Basin, southeastern Austral..., Tectonophysics (2012), doi:10.1016/j.tecto.2012.04.007

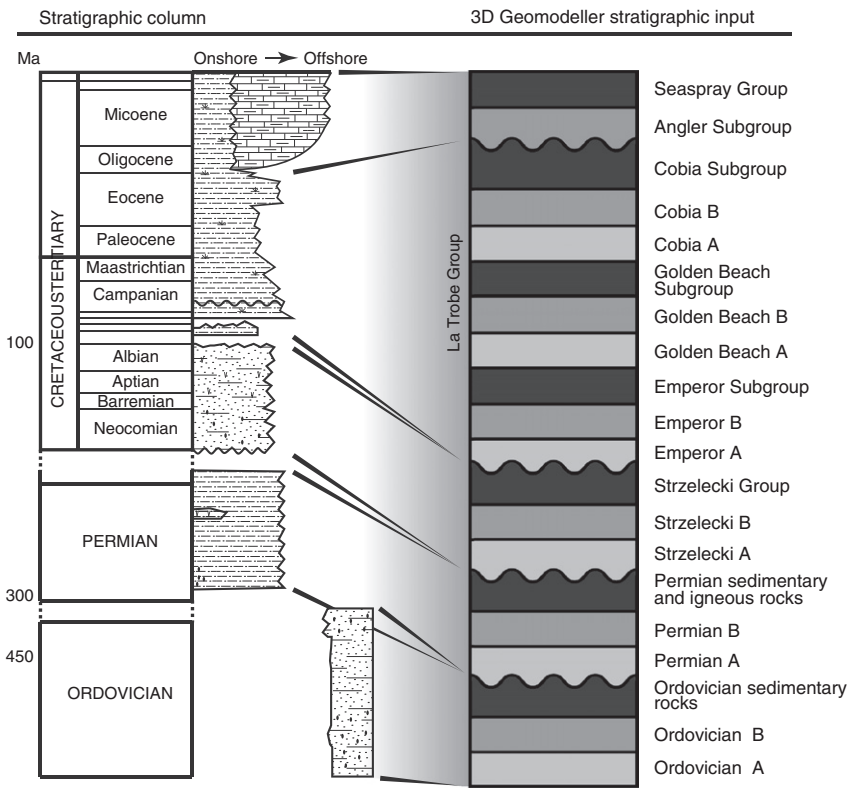

Fig. 10. Gippsland Basin stratigraphic column (adapted from Moore and Wong (2002)) correlated to 3D Geomodeller stratigraphic input. Units with the suffix 'A' and 'B' have been added to increase stratigraphic resolution (Section 6.2.1).

Mapped onshore outcrop information was used in input data; offshore geology was more difficult to constrain and required the use of isopach and bathymetry data combined with seismic interpretation.

6.2.1. Improving the detection of model uncertainty

There are circumstances where uncertain fault surfaces (i.e. poorly constrained fault surface orientations that change due to input data perturbations) are not completely detected. Non-detection occurs if the displacement of the fault is not greater than the thickness of the stratigraphic unit due to the same stratigraphic unit being detected on both the hangingwall and footwall of the fault (Fig. 14). In the example shown in Fig. 14a, the blue unit was assigned a value of one and the white a value of two. The orientation of the fault surfaces does differ from model to model within the model suite, but only a portion of the surface is detected by the technique (Fig. 14b). Different fault locations will not be detected if the stratigraphic unit each side of the fault are the same as only differences in the values assigned to stratigraphic units are detected with this technique. Additional virtual stratigraphic units were added to mitigate these effects (Fig. 14c). Each of these additional virtual units was included in the appropriate 'series', so were included in the implicit potential field calculations of the originating formation. The 3D spatial properties of the virtual units were not treated any differently than the originating unit and were calculated from the same input data.

The practice of adding virtual units increases the 'stratigraphic resolution' of the model, enabling entire uncertain faulting surfaces to be detected when smaller displacements are observed (Fig. 14d). Stratigraphic resolution has been increased in the Gippsland Basin model as some sedimentary layers are thick and fault displacements may not be large enough to avoid the situation described above. Each series has two additional layers added for this purpose, except the top series 'Seaspray_Group', as the thickness of this group is not large enough to warrant additional formations.

6.3. Uncertainty assessment in the Gippsland Basin

Poorly constrained regions and structures in the Gippsland Basin model can be located using methods of uncertainty visualisation. Particular areas of increased uncertainty identified in Fig. 15, highlighted in red on the plan maps, are located in the north (1), northwest (2) and southern parts (3) of the model. Areas (1), (2) and (3) are all associated with faults and the effect of faulting on the cross-cut strata. These faults

Table 2
Input data, purpose and sources.

Data	Purpose	Source
Geophysics — Aeromagnetics and gravity	Geological interpretation of faults	Geoscience Australia
Geophysics — 2D seismic	Geological interpretation of faults and stratigraphy	Geoscience Victoria — Department of Primary Industries
Isopach maps	Constraints for stratigraphic horizons	Geoscience Victoria — Department of Primary Industries
Bathymetry observations	Constraints for stratigraphic horizons	Geoscience Australia
Geological maps	Constraints for onshore outcrop geology Stratigraphic column	Geoscience Victoria — Department of Primary Industries
Stratigraphy	Development of stratigraphic pile	Literature (see references listed in Section 6.1)

Please cite this article as: Lindsay, M.D., et al., Locating and quantifying geological uncertainty in three-dimensional models: Analysis of the Gippsland Basin, southeastern Austral..., Tectonophysics (2012), doi:10.1016/j.tecto.2012.04.007

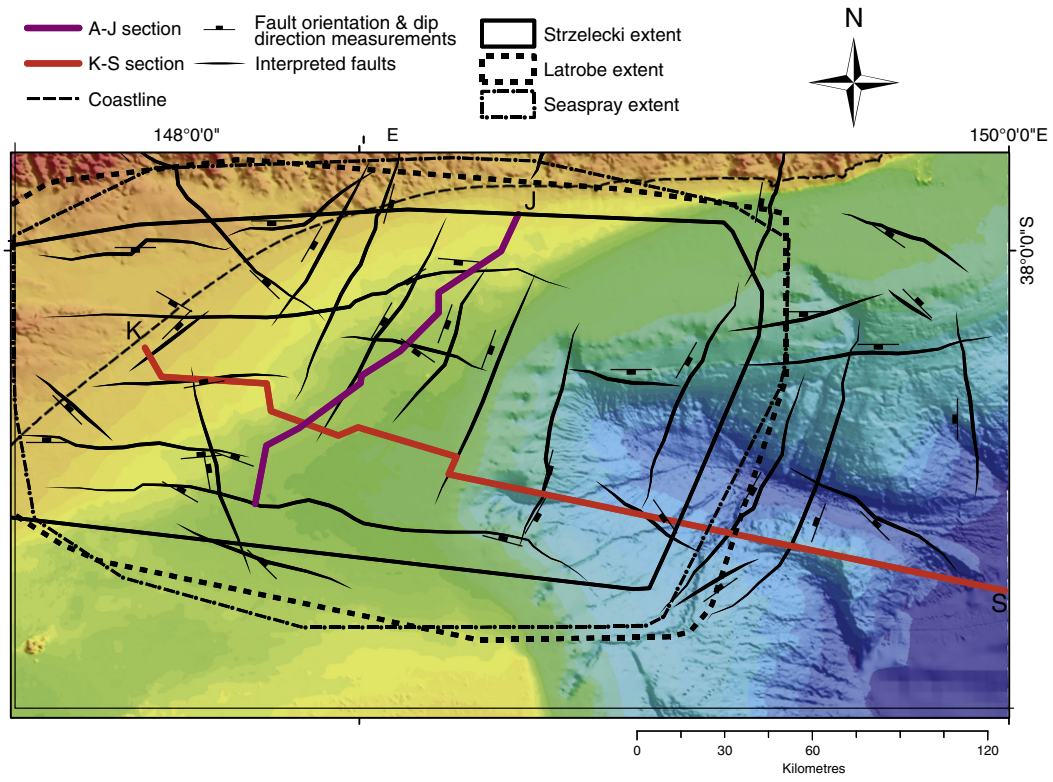

Fig. 11. Location and distribution of input data. Fault and dips interpreted from potential field data (Fig. 13) are overlain on gridded bathymetry data. The extents of isopach information, depicting the tops of three major stratigraphic formations are outlined. Location of seismic sections A–J and K–S are shown blue and red respectively. (For interpretation of the references to colour in this figure legend, the reader is referred to the web version of this article.)

are not well constrained by orientation measurements as they are based on (i) one orientation measurement, (ii) the relationship they have with other faults (i.e. whether they cross-cut or are cross-cut by other faults) and (iii) whether they are defined in the seismic cross-sections K–S. The elongate region of uncertainty running with an east–west axis, just south of the seismic section (region '3') is not defined in the section itself, so does not benefit from any cross-section constraints. The result is that the geology is allowed to vary to a larger degree, displaying higher associated uncertainty values than geology that is represented in the cross-sections.

There are also lack of orientation measurements constraining stratal geometry and distribution in regions of high uncertainty. Onshore observations that we could confidently relate to offshore components are rare and generally relate to formations older than the model basement. In addition, the combined isopach and bathymetry data inputs are largely clustered in the centre and eastern areas of the model, leaving the west relatively unconstrained (Fig. 11). Strata in the uncertain areas rely heavily on the seismic section K–S due to the absence of other data. The over-reliance on section K–S to constrain geological surfaces due to sparse data can also been seen in the northern part of the map where high uncertainty values are observed. Region 2 displays levels of uncertainty due to both high degrees of faulting and the lack of seismic data that could add geometrical constraints to these at depth.

An area of high uncertainty located on the 4000 m depth plan section view of Case Study A (region '4') is due to the intersection of a number of faults and structural complexity resulting from the interaction of strata and the Central Deep. Picking tops from the seismic data of the Strzelecki, Emperor and Golden Beach subgroups in this region was considered 'arbitrary' by Moore and Wong (2002). Estimates of the tops were made based on an interpretation that the Emperor Subgroup thickens to the north and the Strzelecki and Golden Beach Subgroups thicken to the south. It seems that the seismic horizon interpretations do not necessarily correlate to the isopach data. This has resulted in modelled surfaces that vary considerably across the model suite as the implicit potential field method attempts to reconcile the seismic and isopach data. Added complications may have arisen from depth-conversion of two-way-time (TWT) data. Errors in depth-converting TWT data are likely to affect the entirety of this model as it is notoriously difficult to perform without incorporating some error (Cameron, 2007; Suzuki et al., 2008). Time–depth curves of wells were used by Moore and Wong (2002) to determine a seismic velocity model to calculate depth values. Five average internal velocities were used to represent entire density variation of the Gippsland Basin. Local rock density heterogeneity will not be accommodated if bulk density values are assumed. Subsequently some regions of the study area will be mis-represented where local density variations differ from the global averages determined in the velocity model. The result is that horizons interpreted in regions of anomalously high or low density values (with respect to the global average) will not be correctly located spatially. It is most likely that the source of disagreement between data types is caused by a combination of interpretive and data-conversion difficulties.

None of these issues were entirely unexpected in the construction of this model. It was expected that some disagreement between model realisations would be present, given the data types and relative geological complexity. What is important is that the degree and location of disagreement can be shown by detecting the uncertainty in the model. It was subsequently decided that an additional seismic section should be added in an attempt to better constrain the regions of high uncertainty.

6.4. The benefit of additional information

Seismic sections A–J from the Moore and Wong (2002) study were added to the model, an incarnation named Case Study B. Sections A–J start in the southwestern quadrant of the model and extend northeast, intersecting sections K–S just west of the model centre, stopping in the

Please cite this article as: Lindsay, M.D., et al., Locating and quantifying geological uncertainty in three-dimensional models: Analysis of the Gippsland Basin, southeastern Austral..., Tectonophysics (2012), doi:10.1016/j.tecto.2012.04.007

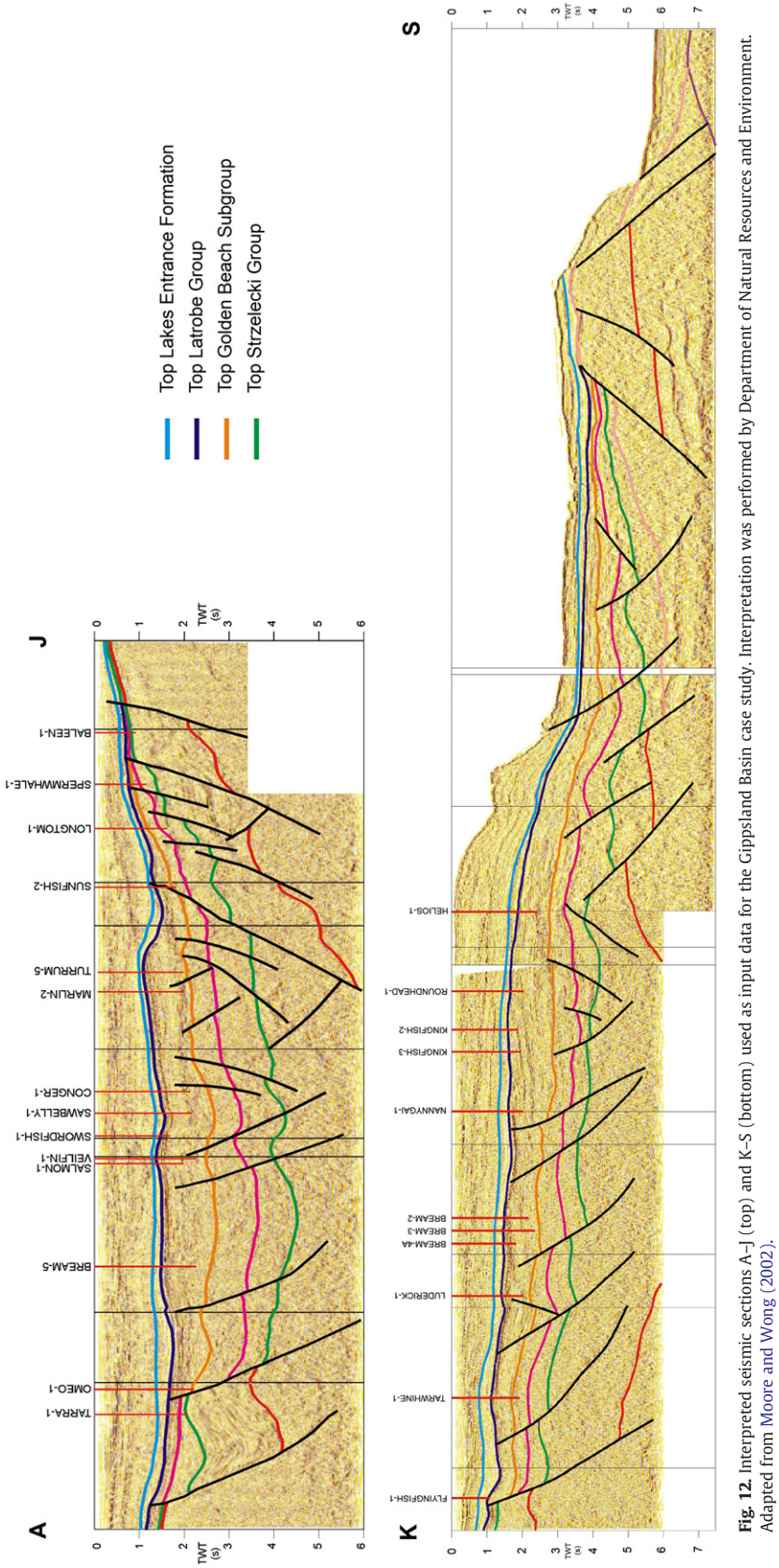

Fig. 12. Interpreted seismic sections A–J (top) and K–S (bottom) used as input data for the Gippsland Basin case study. Interpretation was performed by Department of Natural Resources and Environment. Adapted from Moore and Wong (2002).

Please cite this article as: Lindsay, M.D., et al., Locating and quantifying geological uncertainty in three-dimensional models: Analysis of the Gippsland Basin, southeastern Austral..., Tectonophysics (2012), doi:10.1016/j.tecto.2012.04.007

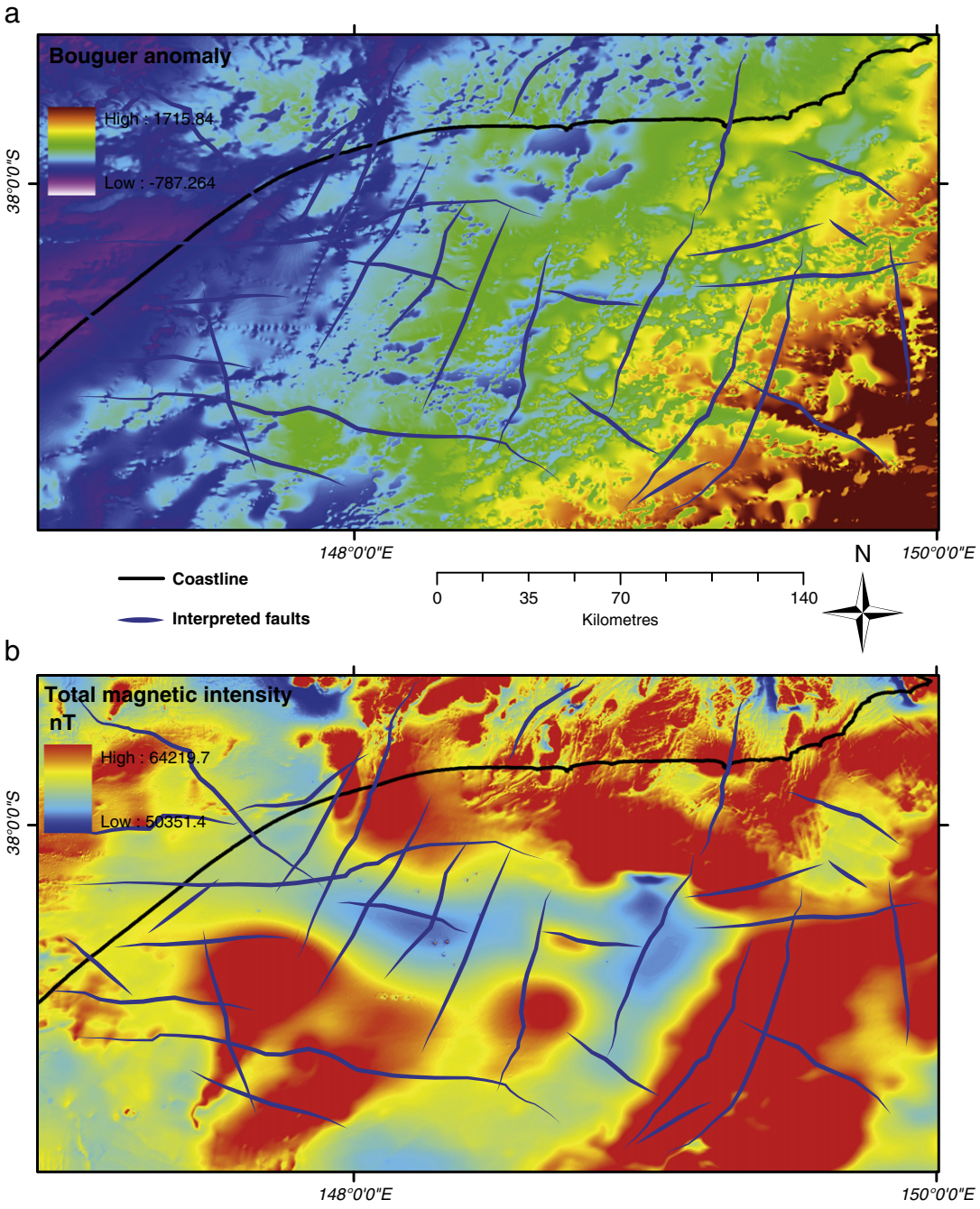

Fig. 13. Interpreted geophysical potential field datasets used as input for the Gippsland Basin case study. (a) Bouguer gravity anomaly shown with a southeast directed 'hillshade' effect for enhancement. (b) Total magnetic intensity anomaly shown with no 'hillshade' effect.

northern centre (Fig. 11). The results in removing uncertainty can be seen qualitatively in the Case Study B maps (Fig. 15). Uncertainty in the northern region of interest (1) has been significantly reduced in Case Study B and areas (2) and (4) have also been reduced, but to a lesser extent. Region (3) still displays a high degree of uncertainty, though it has been reduced below that displayed in Case Study A.

Change in uncertainty is quantified by calculating the difference in volume for different L values ($L=2$, 4 and 6) (Fig. 16). The differences between these values in Case Study A and Case Study B are also shown. The differences equate to a percentage decrease of 64.5 ($L=2$), 53.7 ($L=4$) and 87.5 ($L=6$), showing that adding seismic sections A–J to the model improved the potential for geology to be more reliably modelled.

6.5. Discrete regions of uncertainty

Overall improvements to model uncertainty were addressed by adding additional information to the model. There remain regions of high uncertainty within the model (Fig. 15, region '5') in the Central Deep. One explanation is that there is no isopach information to aid strata geometry. Most of the information in this region is defined by the seismic section R–S and fault interpretations made from geophysical potential field data or seismic interpretation. This is compounded by difficulties in seismic interpretation of formation tops in the Gippsland Deep (Moore and Wong, 2002). It is clear that there are issues when attempting to correlate faults interpreted by geophysical potential fields to those interpreted from seismic data. Uncertain regions are

Please cite this article as: Lindsay, M.D., et al., Locating and quantifying geological uncertainty in three-dimensional models: Analysis of the Gippsland Basin, southeastern Austral..., Tectonophysics (2012), doi:10.1016/j.tecto.2012.04.007

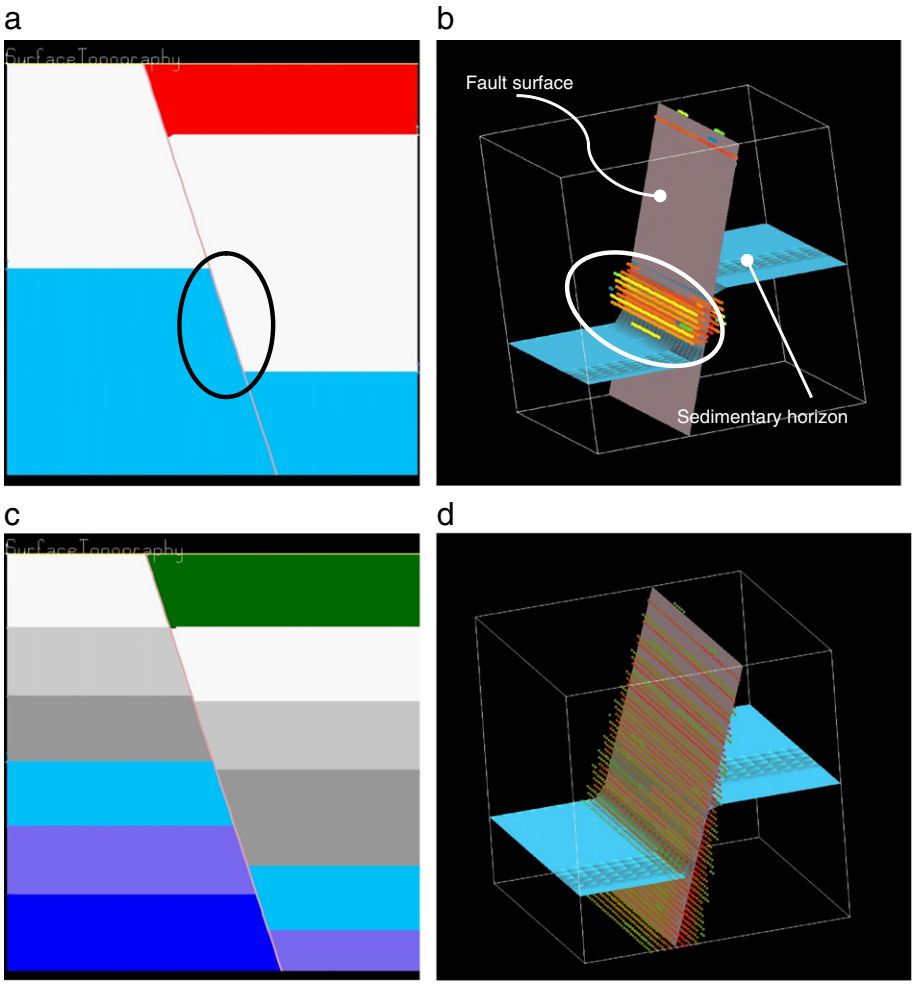

Fig. 14. When fault displacement is less than stratigraphic thickness fault surfaces may not be completely detected. This example shows a modelled normal fault represented in section view (left) and in 3D on the right. Note that only where the blue and white units (circled — left) are adjacent is there the possibility of uncertainty (shown with point data) being detected (circled — right). With the addition of virtual formations (c) the uncertainty along the entire fault surface can be resolved (d). (For interpretation of the references to colour in this figure legend, the reader is referred to the web version of this article.)

generated by using ambiguous input data during model construction. This is true for geophysical data, in terms of non-unique solutions for geophysical potential field interpretation and the aforementioned issues relating to seismic data interpretation and integration into a 3D model. While it is tempting to avoid using geophysical data to prevent the possibility of making ambiguous observations, is it not feasible. Problems of sparse data require the use of geophysics in regional scales studies, such as that undertaken by Moore and Wong (2002). The key is locating, mitigating and understanding the nature of model uncertainty.

7. Discussion

The method presented here has shown it is possible to locate and calculate the magnitude of uncertainty within a 3D model of real geology. The method has allowed assessment of the Gippsland Basin model for inherent uncertainties and has aided the identification of data sources that may disagree. It appears that constraining the geology in central parts and an eastern region of the basin is particularly problematic due to heavy reliance on difficult to interpret seismic information. Additional information can provide geological constraints that reduce uncertainty, as has been shown. Consideration must be made that new information may also introduce additional uncertainty. The disagreement between the isopach-derived and interpreted seismic data, an occurrence not uncommon in basin studies (Suzuki et al., 2008), highlights how different data types do not necessarily reduce uncertainty by constraining each other, but create a situation where uncertainty is increased. Therefore it is likely the degree of geological complexity in the northwestern, central and eastern regions of the model is higher than that which can be interpolated using the current data inputs.

Stratigraphic variability values provide the operator with an intuitive method with which to understand two fundamental, but separate, components of model uncertainty: stratigraphic possibility (L) and stratigraphic variability frequency (P). These concepts are simple, easy to calculate and meaningful to the non-expert. Both the normalised stratigraphic possibility and variability values are model independent and do not require redefining for different geological settings. Both values are calculated from statistical methods, so are therefore repeatable and objective. This method also generates a variety of model perturbations in the process of determining uncertainty that can be assessed individually to provide an expanded view of what may be possible geologically.

It is important that the information generated by this technique is presented with an appropriate visualisation tool to adequately communicate the complexities of model uncertainty to the operator (Gershon, 1998; Thomson et al., 2005). Other effective methods of uncertainty visualisation exist (MacEachren et al., 1998; Viard et al., 2010; Wellmann and Regenauer-Lieb, 2011; Zuk and Carpendale, 2006) and have been considered for the purposes of this technique. The 'heat-map' colour scheme has been chosen because it is intuitive

Please cite this article as: Lindsay, M.D., et al., Locating and quantifying geological uncertainty in three-dimensional models: Analysis of the Gippsland Basin, southeastern Austral..., Tectonophysics (2012), doi:10.1016/j.tecto.2012.04.007

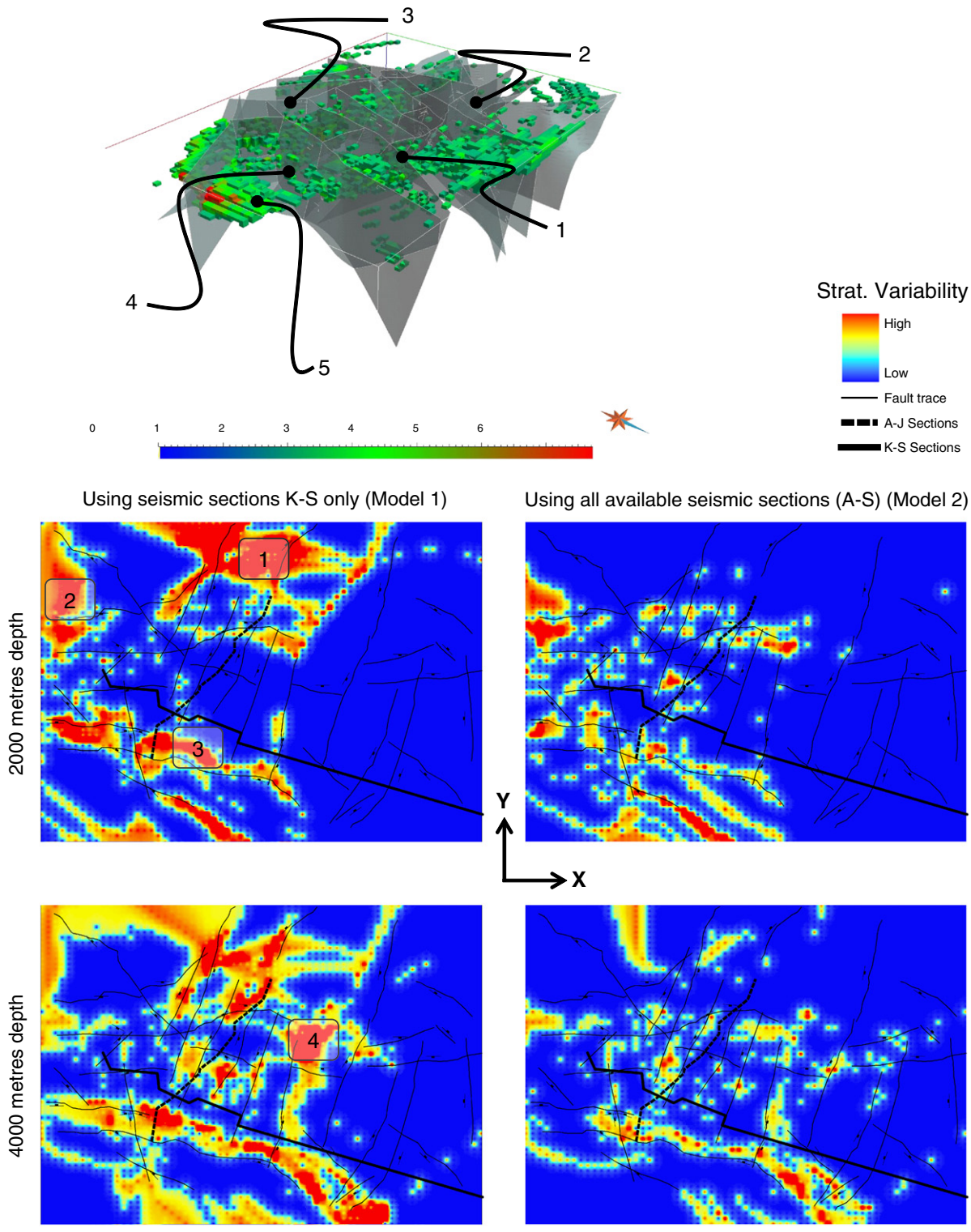

Fig. 15. Comparison of stratigraphic variability observed at 2000 m and 4000 m depth. All maps are in plan view. Note areas of high stratigraphic variability (uncertainty) located to the north, northwest and southwest of Case Study A. Labelled regions are correspondingly labelled in the 3D view of uncertainty (voxet model, $L \geq 2$, grey surfaces are faults). Significant improvements to uncertainty values have been made in these areas with the addition seismic section information in Case Study B. Another interesting feature is the association of uncertainty with the faults and in some cases the dip of the fault can be determined by the uncertainty gradient. For example, the east–west fault in the south of the map shows a northerly dip, which is confirmed by associated strike and dip orientations. (For interpretation of the references to colour in this figure legend, the reader is referred to the web version of this article.)

for most geoscientists and allows an appropriate amount of colour variation to effectively show the attributed quantities. The magnitude of uncertainty is directly related to colour and variations in data are clear to the operator. Regions of uncertainty are then identified using a combination of point data and stratigraphic variability values assigned to a colour map. Thresholds can be applied to the colour map

Please cite this article as: Lindsay, M.D., et al., Locating and quantifying geological uncertainty in three-dimensional models: Analysis of the Gippsland Basin, southeastern Austral..., Tectonophysics (2012), doi:10.1016/j.tecto.2012.04.007

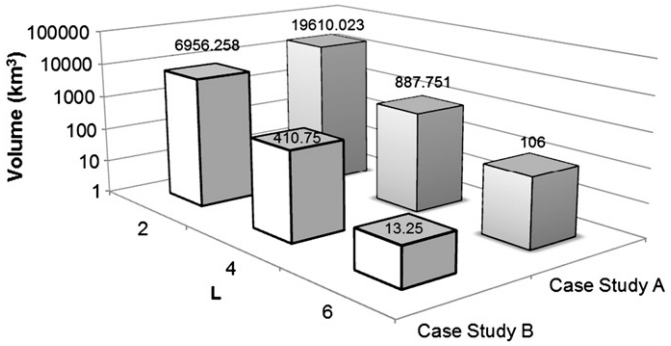

Fig. 16. Change in uncertainty due to additional data. Volumes of stratigraphic possibilities (L) have been separated into three thresholds representing low ($L \geq 2$), medium ($L \geq 4$) and high ($L \geq 6$) levels of uncertainty. Levels of uncertainty contained within model Case Study A to Case Study B are plotted against a logarithmic volume scale (km^3). Reductions in uncertainty seen between Case Study A and Case Study B are due to the addition of seismic section information.

to delineate high or low ranges of uncertainty. The features of stratigraphic variability allow the spatial variation of uncertainty and associated geological elements to be easily identified.

Another means to visualise model uncertainty is provided by assigning stratigraphic variability values to voxets. The use of voxets also allows the calculation of uncertainty volumes, in contrast Wellmann et al. (2010) who focus on visualising uncertainty with surfaces. Knowledge of uncertainty volumes provides a particularly useful comparative measure for assessing uncertainty between different model versions or quantifying the effect of additional data sets on model iterations. Importantly for this study, uncertainty volumes provide a descriptive quantity that can be used for reporting purposes when reviewing a model for reliably representing a geological target.

A different method to quantify uncertainty has been suggested by Jessell et al. (2010) that employs a distance penalty function applied to the model suite where stratigraphic observations are compared against predictions. The closest modelled location(s) sharing the same properties as an observation point are determined and Euclidean distance is calculated. The results provide a distance misfit error that describes the geological variability of a model suite within a local area. The benefit to using this method is that stratigraphic units can be reclassified into ordinal data and subdomains of related geological units can be defined. The results can then be subjected to a wider range of statistical treatments. Additional measures derived from different statistics would be advantageous to detecting and quantifying uncertainty. A drawback to using distance misfit error is that only uncertainty contained within a local area is measured, whereas the stratigraphic variability describes uncertainty at a discrete location. In addition, adjusting the method for this technique to a local area distance calculation presents a challenge in how to define an 'observed' location or the reference model itself. This paper defines the 'reference model' as that which is produced using unperturbed orientation measurements. This definition of a reference model is not an unbiased estimate, as it depends on the internal parameterisation of the implicit scheme applied. Another definition for a reference model could be the 'mode model', as it represents the most common stratigraphic units for every given point across the model suite. The mode model incorporates all the perturbed orientation datasets, not just a single orientation dataset, and accommodates more geological possibility. The mode model is derived statistically from a voxet and does not necessarily retain any geological connectivity or feasibility. A solution to this problem is to find a model in the model suite that corresponds exactly to the mode model, which, if it exists, could be legitimately classified as the reference model.

Multiple realisations of a single geological concept are being analysed in this study. Multiple realisations of multiple geological concepts can be analysed if topological relationships are varied in combination with orientation observations. The implicit method requires topological input in the form of a stratigraphic column (with appropriate 'onlap' or 'erode' relationships between units), a defined fault network and fault–stratigraphy relationships. If any topological relationships are perturbed, fundamental changes to the model will occur and produce far greater variability in the model suite than if, as in this study, only the input orientation observations are perturbed. There is good reason to perform topological perturbation. Most geological terranes have multiple tectonic evolution hypotheses and could be comparatively tested using topological perturbation. Appropriate analysis of these results would require the process to reject models on the basis of geological impossibility, a concept that is open to vigorous debate. The boundaries of model space are greatly expanded by allowing topological perturbation and more degrees of freedom, requiring increased model suite members and subsequently requiring faster model calculation and sampling. These are minor challenges to resolve when considering the benefits. Geological possibility, and therefore uncertainty, is not being fully explored if different model topologies are not included in analysis.

The production of a model suite and uncertainty analysis has an additional educational application. Generating multiple models can aid management decisions and educate non-geoscientists. The degree of variation observed between models due to small perturbations of the input data highlight the problems of sparse data inherent in geosciences. These concepts are often not well acknowledged outside of scientific disciplines like geosciences and astronomy. One of the conclusions from the Bond et al. (2010) study was that to better prepare geoscience students for professional life, discouragement of striving to find the 'best' answer and accepting multiple answers needs to be effectively communicated. This conclusion can also be applied to management personnel that have not been trained within the geosciences. Acknowledgement that a single 'correct' answer is not necessarily available can be aided by this technique by visualising the degree of uncertainty within a particular model.

7.1. Improving understanding of model uncertainty

Improvements can be made to better assess uncertainty contained within 3D models. There are possible augmentations to this technique that may offer more information to the operator.

a) Higher resolution sampling. Model sampling parameters used in this study can be improved in two ways. A vertical bias exists as the sampling interval on the Z axis is 500 m, whereas on the X and Y axes it is 4140.625 m and 3200 m respectively. It would be preferable to have all axes equal to ensure no directional bias exists and to have smaller intervals to ensure that the geometry of inherent uncertainty can be more accurately defined. The restriction in this case was due to hardware requirements. The assessment was conducted on a personal laptop (250GB HDD) and smaller sampling is restricted heavily by hard disk space. It would be preferable for future studies to be conducted on high-capacity computing platforms to address this.
b) Use of continuous variables. The stratigraphic identifier used in this study to describe the stratigraphic unit at a given point returns a categorical variable. As such, there are limited statistical treatments that are available for analysis. One solution would be to identify both the type of stratigraphy (currently done) and the implicit potential field value the model is interpolated with. The implicit potential field value is a continuous variable and would give a value revealing where sample location is in the stratigraphic unit and proximity to other geological interfaces (contacts, faults). This information would very useful in terms of developing better techniques to analyse, visualise and use uncertainty data to improve model reliability. It would also remove

Please cite this article as: Lindsay, M.D., et al., Locating and quantifying geological uncertainty in three-dimensional models: Analysis of the Gippsland Basin, southeastern Austral..., Tectonophysics (2012), doi:10.1016/j.tecto.2012.04.007

the need to add additional formations to increase stratigraphic resolution.

c) Calculation of stratigraphic distance. Accommodating uncertainty between both stratigraphy and lithology can be achieved with the use of a weighting schema and additional information from the 3D Geomodeller implicit potential field. Currently no consideration of geochronology and unconformable relationships is made when calculating uncertainty. Locations which display lithological variability within the same stratigraphic group, such as variation between the Angler Subgroup and the Seaspray Group (both part of the Seaspray Series) (Fig. 10) could have a lesser weighting than variability between the Angler Subgroup (Seaspray Group Series) and the Cobia Subgroup (Latrobe Group Series). This difference in weighting can be justified as an erosional unconformity that separates the Angler and Cobia units, whereas the Angler and Seaspray units are generally considered to be conformable. Knowledge of the implicit potential field value and gradient would be beneficial to accurately calculate stratigraphic distance. The implicit potential field value would allow calculation of Euclidian distance in three dimensions, as the position within stratigraphy would be known. The implicit potential field gradient value would assist in describing the direction of stratigraphic anisotropy within the geological layer and from this the orientation of the stratigraphic distance vector could be found.

7.2. Geological constraints for geophysical inversion

Calculating stratigraphic variability produces information that could potentially provide geological constraints for geophysical inversion. Current inversion techniques provide geological constraints in the form of petrophysical rock property distributions (Guillen et al., 2008; Jessell et al., 2010; Li and Oldenburg, 1998), 'pierce points' assigned to stratigraphic horizons in drill-holes (Fullagar et al., 2000) or weightings applied to entire surfaces (Fullagar et al., 2008) that restrict movement during geometrical inversion. However, existing techniques do not integrate all available geological data into the process, such as orientation measurements, and therefore cannot be expected to honour all data inputs. The information provided by this technique could offer a method to constrain the geophysical inversion process. Both L and P values, together representing stratigraphic variability, could provide an adjustment threshold for cells during inversion. If the possible cell solutions are limited to what is defined by their associated L and P values, then the final inverted model will more likely to represent a realistic geological situation as it honours all the data.

For example, if $L=3$ and $P=0.23$ for a cell at X, Y, Z, then the inversion process would be limited to varying the cell to the three possible stratigraphic units identified by this technique. The 0.23 P value, indicating what frequency the stratigraphic unit differs from the mode, can be used as a weighting coefficient representing the likelihood of this cell being changed during inversion. A consideration in using stratigraphic variability as a constraint to geophysical inversion is that the process may fail and render no result, which is potentially more useful than if the process completes successfully. A failed inversion executed with these geological constraints as input would suggest that the geological reference model, input data and the geophysical data used in the inversion may differ to a degree beyond what geologically feasible.

8. Conclusion

Uncertainty in 3D geological models can be located, visualised and quantified in the pursuit of building a reliable 3D geological model. Uncertainty can be used to identify potentially unreliable regions in 3D models, requiring additional data constraints. Reduction of uncertainty is also measurable, and can be used to explore whether adding more data is beneficial. A principal assumption in this study is that the input data, potentially of high quality, is not without error. Attempts to correct the data and remove error are not performed. Instead this study offers a process where a suite of geological possibilities can be generated from a single input data set through perturbations of the data. Significant reductions of model uncertainty can be achieved by using appropriate data in key locations within the 3D model. The location and magnitude of uncertainty also reveal regions that bear further geological or geophysical analysis. Uncertain regions can be treated by adding more data, or may guide future surveys and studies if data is unavailable. Producing an uncertainty grid and stratigraphic variability values is a step towards the goal of a geophysically and geologically constrained inversion process that produces models that honour both geophysical and geological data.

Acknowledgements

We gratefully acknowledge the assistance of the team at Intrepid Geophysics, Melbourne, Australia, who supplied the 3D Geomodeller API and provided technical support. This study would not have been possible without financial support and datasets supplied by Tim Rawling and Geoscience Victoria, Department of Primary Industries, Melbourne, Australia. We would also like to thank the Society of Economic Geologists and the Hugo Dummett Memorial Fund for awarding funding in support of this study. Finally, we acknowledge the thorough and constructive feedback provided by two anonymous reviewers and Alan Gibbs of Midland Valley.

References

Agresti, A., 2007. An Introduction to Categorical Data Analysis, 2nd ed. John Wiley & Sons, Inc., Hoboken, New Jersey.

Aitken, A.R.A., Betts, P.G., 2009. Multi-scale integrated structural and aeromagnetic analysis to guide tectonic models: an example from the eastern Musgrave Province, Central Australia. Tectonophysics 476, 418–435.

Bernecker, T., Partridge, A.D., 2001. Emperor and Golden Beach Subgroups: the onset of Late Cretaceous sedimentation in the Gippsland Basin. In: Hill, K.C., Bernecker, T. (Eds.), Eastern Australian Basins Symposium, a refocused energy perspective for the future: Petroleum Exploration Society of Australia, Special Publication, pp. 391–402.

Bernecker, T., Woollands, M., Wong, D., Moore, D., Smith, M., 2001. Hydrocarbon prospectivity of the deep water Gippsland Basin, Victoria, Australia. APPEA Journal 41, 91–113.

Betts, P.G., Valenta, R.K., Finlay, J., 2003. Evolution of the Mount Woods Inlier, northern Gawler Craton, Southern Australia: an integrated structural and aeromagnetic analysis. Tectonophysics 366, 83–111.

Bond, C.E., Philo, C., Shipton, Z.K., 2010. When there isn't a right answer: interpretation and reasoning, key skills for twenty-first century geoscience. International Journal of Science Education 33, 629–652.

Bowden, R.A., 2007. Sources of uncertainty in the estimation and reporting of results from down hole gamma-ray and prompt fission neutron logging for uranium. Australasian Institute of Mining and Metallurgy Publication Series.

Calcagno, P., Chilès, J.P., Courrioux, G., Guillen, A., 2008. Geological modelling from field data and geological knowledge: part I. modelling method coupling 3D potential-field interpolation and geological rules. Physics of the Earth and Planetary Interiors 171, 147–157.

Cameron, M.K., 2007. Seismic velocity estimation from time migration. Inverse Problems 23, 1329–1369.

Caumon, G., Tertois, A.-L., Zhang, L., 2007. Elements for stochastic structural perturbation of stratigraphic models. Proceedings of Petroleum Geostatistics. EAGE.

Clark, D.A., 1983. Comments on magnetic petrophysics. Bulletin of the Australian Society of Exploration Geophysicists 14, 49–62.

Clark, D.A., 1997. Magnetic petrophysics and magnetic petrology: aids to geological interpretation of magnetic surveys. AGSO Journal of Australian Geology and Geophysics 17, 83–103.

Cook, P.J., 2006. Carbon dioxide capture and geological storage: research, development and application in Australia. International Journal of Environmental Studies 63, 731–749.

Davis, J.C., 2002. Statistics and Data Analysis in Geology, Third ed. Wiley, New York.

Fullagar, P.K., Hughes, N.A., Paine, J., 2000. Drilling-constrained 3D gravity interpretation. Exploration Geophysics 31, 017–023.

Fullagar, P.K., Pears, G.A., McMonnies, B., 2008. Constrained inversion of geologic surfaces — pushing the boundaries. The Leading Edge 27, 98–105.

Gallagher, S.J., Smith, A.J., Jonasson, K., Wallace, M.W., Holdgate, G.R., Daniels, J., Taylor, D., 2001. The Miocene palaeoenvironmental and palaeoceanographic evolution of the Gippsland Basin, Southeast Australia: a record of Southern Ocean change. Palaeogeography, Palaeoclimatology, Palaeoecology 172, 53–80.

Gershon, N., 1998. Visualization of an imperfect world. IEEE Computer Graphics and Applications 18, 43–45.

Please cite this article as: Lindsay, M.D., et al., Locating and quantifying geological uncertainty in three-dimensional models: Analysis of the Gippsland Basin, southeastern Austral..., Tectonophysics (2012), doi:10.1016/j.tecto.2012.04.007

Grant, F.S., 1985. Aeromagnetics, geology and ore environments, I. magnetite in igneous, sedimentary and metamorphic rocks: an overview. Geoexploration 23, 303–333.
Gray, D.R., Foster, D.A., 1998. Character and kinematics of faults within the turbidite-dominated Lachlan Orogen: implications for tectonic evolution of eastern Australia. Journal of Structural Geology 20, 1691–1720.
Guillen, A., Calcagno, P., Courrioux, G., Joly, A., Ledru, P., 2008. Geological modelling from field data and geological knowledge: part II. modelling validation using gravity and magnetic data inversion. Physics of the Earth and Planetary Interiors 171, 158–169.
Gunn, P.J., 1997. Quantitative methods for interpreting aeromagnetic data: a subjective review. AGSO Journal of Australian Geology and Geophysics 17, 105–114.
Gunn, P.J., Maidment, D., Milligan, P.R., 1997. Interpreting aeromagnetic data in areas of limited outcrop. AGSO Journal of Australian Geology and Geophysics 17, 175–185.
Haq, B.U., Hardenbol, J., Vail, P.R., 1987. Chronology of fluctuating sea levels since the Triassic. Science 235, 1156–1167.
Holdgate, G.R., Gallagher, S.J., Wallace, M.W., 2002. Tertiary coal geology and stratigraphy of the Port Phillip Basin, Victoria. Australian Journal of Earth Sciences 49, 437–453.
Jessell, M., 2001. Three-dimensional geological modelling of potential-field data. Computers & Geosciences 27, 455–465.
Jessell, M.W., Ailleres, L., de Kemp, E.A., 2010. Towards an integrated inversion of geoscientific data: what price of geology? Tectonophysics 490, 294–306.
Joly, A., Chen, Y., Faure, M., Martelet, G., 2007. A multidisciplinary study of a syntectonic pluton close to a major lithospheric-scale fault — relationships between the Montmarault granitic massif and the Sillon Houiller Fault in the Variscan French Massif Central: 1. geochronology, mineral fabrics, and tectonic implications. Journal of Geophysical Research 112.
Joly, A., Martelet, G., Chen, Y., Faure, M., 2008. A multidisciplinary study of a syntectonic pluton close to a major lithospheric-scale fault — relationships between the Montmarault granitic massif and the Sillon Houiller Fault in the Variscan French Massif Central: 2. gravity, aeromagnetic investigations, and 3-D geologic modeling. Journal of Geophysical Research 113.
Jones, R.R., McCaffrey, K.J.W., Wilson, R.W., Holdsworth, R.E., 2004. Digital field data acquisition: towards increased quantification of uncertainty during geological mapping. Geological Society, London, Special Publications 239, 43–56.
Kaufmann, O., Martin, T., 2008. 3D geological modelling from boreholes, cross-sections and geological maps, application over former natural gas storages in coal mines. Computers & Geosciences 278–290.
Lajaunie, C., Courrioux, G., Manuel, L., 1997. Foliation fields and 3D cartography in geology: principles of a method based on potential interpolation. Mathematical Geology 29, 571–584.
Li, Y., Oldenburg, D.W., 1998. 3-D inversion of gravity data. Geophysics 63, 109–119.
MacEachren, A.M., Brewer, C.A., Pickle, L.W., 1998. Visualizing georeferenced data: representing reliability of health statistics. Environment and Planning A 30, 1547–1561.
Mallet, J.L., 1992. Discrete smooth interpolation in geometric modelling. Computer-Aided Design 24, 178–191.
Mitchell, J.K., Holdgate, G.R., Wallace, M.W., 2007. Pliocene–Pleistocene history of the Gippsland Basin outer shelf and canyon heads, southeast Australia. Australian Journal of Earth Sciences: An International Geoscience Journal of the Geological Society of Australia 54, 49–64.
Moore, D., Wong, D., 2002. Eastern and Central Gippsland Basin, Southeast Australia. Basement Interpretation and Basin Links, Victorian Initiative for Minerals and Petroleum Report 69. Department of Natural Resources and Environment.
Nabighian, M.N., Grauch, V.J.S., Hansen, R.O., LaFehr, T.R., Li, Y., Peirce, J.W., Phillips, J.D., Ruder, M.E., 2005. The historical development of the magnetic method in exploration. Geophysics 70, 33ND–61ND.
Nettleton, L.L., 1942. Gravity and magnetic calculations. Geophysics 7, 293–310.
Polanyi, M., 1962. Tacit knowing: its bearing on some problems of philosophy. Reviews of Modern Physics 34, 601–616.
Putz, M., Stüwe, K., Jessell, M., Calcagno, P., 2006. Three-dimensional model and late stage warping of the Plattengneis Shear Zone in the Eastern Alps. Tectonophysics 412, 87–103.
Rahmanian, V.D., Moore, P.S., Mudge, W.J., Spring, D.E., 1990. Sequence stratigraphy and the habitat of hydrocarbons, Gippsland Basin, Australia. Geological Society, London, Special Publications 50, 525–544.
Royse, K.R., 2010. Combining numerical and cognitive 3D modelling approaches in order to determine the structure of the Chalk in the London Basin. Computers & Geosciences 36, 500–511.
Schmidt, P.W., McDougall, I., 1977. Palaeomagnetic and potassium–argon dating studies of the Tasmanian Dolerites. Journal of the Geological Society of Australia 24, 321–328.
Singer, D., Menzie, W., 2010. Quantitative Mineral Resource Assessments: An Integrated Approach. Oxford University Press.
Smith, M.A., Bernecker, T., Liberman, T., Moore, D., Wong, D., 2000. Petroleum prospectivity of the deep-water gazettal areas V00-3 and V00-4, southeastern Gippsland Basin, Victoria, Australia. Victorian Initiative for Minerals and Petroleum. Department of Natural Resources and Environment.
Suzuki, S., Caumon, G., Caers, J., 2008. Dynamic data integration for structural modeling: model screening approach using a distance-based model parameterization. Computational Geosciences 12, 105–119.
Thomson, J., Hetzler, E., MacEachren, A., Gahegan, M., Pavel, M., 2005. A typology for visualizing uncertainty. Proceedings of SPIE — The International Society for Optical Engineering, pp. 146–157.
Thore, P., Shtuka, A., Lecour, M., Ait-Ettajer, T., Cognot, R., 2002. Structural uncertainties: determination, management, and applications. Geophysics 67, 840–852.
Torvela, T., Bond, C.E., 2010. Do experts use idealised structural models? Insights from a deepwater fold-thrust belt. Journal of Structural Geology 33, 51–58.
Veevers, J.J., 1986. Breakup of Australia and Antarctica estimated as mid-Cretaceous (95 ± 5 Ma) from magnetic and seismic data at the continental margin. Earth and Planetary Science Letters 77, 91–99.
Veevers, J.J., Powell, C.M., Roots, S.R., 1991. Review of seafloor spreading around Australia. I. Synthesis of the patterns of spreading. Australian Journal of Earth Sciences: An International Geoscience Journal of the Geological Society of Australia 38, 373–389.
Viard, T., Caumon, G., Lévy, B., 2010. Adjacent versus coincident representations of geospatial uncertainty: which promote better decisions? Computers & Geosciences 37, 511–520.
Wellmann, J.F., Regenauer-Lieb, K., 2011. Uncertainties have a meaning: information entropy as a quality measure for 3-D geological models. Tectonophysics 526–529, 207–216.
Wellmann, F.J., Horowitz, F.G., Schill, E., Regenauer-Lieb, K., 2010. Towards incorporating uncertainty of structural data in 3D geological inversion. Tectonophysics 490, 141–151.
Williams, H.A., Betts, P.G., Ailleres, L., 2009. Constrained 3D modeling of the Mesoproterozoic Benagerie Volcanics, Australia. Physics of the Earth and Planetary Interiors 173, 233–253.
Willman, C.E., VandenBerg, A.H.M., Morand, V.J., 2002. Evolution of the southeastern Lachlan Fold Belt in Victoria. Australian Journal of Earth Sciences 49, 271–289.
Zuk, T., Carpendale, S., 2006. Theoretical analysis of uncertainty visualizations. In: Erbacher, R.F., Roberts, J.C., Gröhn, M.T., Börner, K. (Eds.), Proceedings of SPIE-IT&T Electronic Imaging. SPIE, pp. 66–79.

Please cite this article as: Lindsay, M.D., et al., Locating and quantifying geological uncertainty in three-dimensional models: Analysis of the Gippsland Basin, southeastern Austral..., Tectonophysics (2012), doi:10.1016/j.tecto.2012.04.007